HHS Public Access

Author manuscript

Cell Rep. Author manuscript; available in PMC 2019 May 20.

Published in final edited form as:

Cell Rep. 2019 April 30; 27(5): 1472–1486.e5. doi:10.1016/j.celrep.2019.04.011.

Distinct Requirements of CHD4 during B Cell Development and Antibody Response

Wei-Feng Yen[1,2,8], **Rahul Sharma**[1,8], **Montserrat Cols**[1], **Colleen M. Lau**[1], **Ashutosh Chaudhry**[1], **Priyanka Chowdhury**[1,3], **William T. Yewdell**[1], **Bharat Vaidyanathan**[1,3], **Amy Sun**[4], **Maryaline Coffre**[4], **Joseph N. Pucella**[5], **Chun-Chin Chen**[2,6], **Maria Jasin**[2,5,6], **Joseph C. Sun**[1,3,5], **Alexander Y. Rudensky**[1,3,5,7], **Sergei B. Koralov**[4], and **Jayanta Chaudhuri**[1,3,5,9,*]

[1]Immunology Program, Memorial Sloan Kettering Cancer Center, New York, NY, USA

[2]Biochemistry, Cellular and Molecular Biology Program, Weill Graduate School of Medical Sciences, New York, NY, USA

[3]Immunology and Microbial Pathogenesis Program, Weill Cornell Graduate School of Medical Sciences, New York, NY, USA

[4]Department of Pathology, New York University School of Medicine, New York, NY, USA

[5]Gerstner Sloan Kettering Graduate School of Biomedical Sciences, New York, NY, USA

[6]Developmental Biology Program, Memorial Sloan Kettering Cancer Center, New York, NY, USA

[7]Howard Hughes Medical Institute, Memorial Sloan Kettering Cancer Center, New York, NY, USA

[8]These authors contributed equally

[9]Lead Contact

SUMMARY

The immunoglobulin heavy chain (*Igh*) locus features a dynamic chromatin landscape to promote class switch recombination (CSR), yet the mechanisms that regulate this landscape remain poorly understood. CHD4, a component of the chromatin remodeling NuRD complex, directly binds H3K9me3, an epigenetic mark present at the *Igh* locus during CSR. We find that CHD4 is essential for early B cell development but is dispensable for the homeostatic maintenance of mature, naive B cells. However, loss of CHD4 in mature B cells impairs CSR because of suboptimal targeting of AID to the *Igh* locus. Additionally, we find that CHD4 represses p53 expression to promote B cell proliferation. This work reveals distinct roles for CHD4 in B cell

*Correspondence: chaudhuj@mskcc.org.

AUTHOR CONTRIBUTIONS

W.-F.Y., R.S., M. Cols, C.M.L., A.C., P.C., W.T.Y., B.V., A.S., M. Coffre, S.B.K., and J.C. conceived and designed the experiments. W.-F.Y., R.S., M. Cols, A.C., P.C., W.T.Y., B.V., A.S., M. Coffre, and C.C.C. performed the experiments. W.F.Y., R.S., M. Cols, A.C., P.C., W.T.Y., B.V., A.S., M. Coffre, C. C.C., M.J., J.C.S., S.B.K., A.Y.R., and J.C. analyzed the data. C.M.L. performed bioinformatics analysis. W.F.Y., R.S., M. Cols, W.T.Y., C.M.L., and J.C. wrote the manuscript.

SUPPLEMENTAL INFORMATION

Supplemental Information can be found online at https://doi.org/10.1016/j.celrep.2019.04.011.

DECLARATION OF INTERESTS

The authors declare no competing interests.

development and CSR and links the H3K9me3 epigenetic mark with AID recruitment to the *Igh* locus.

Graphical Abstract

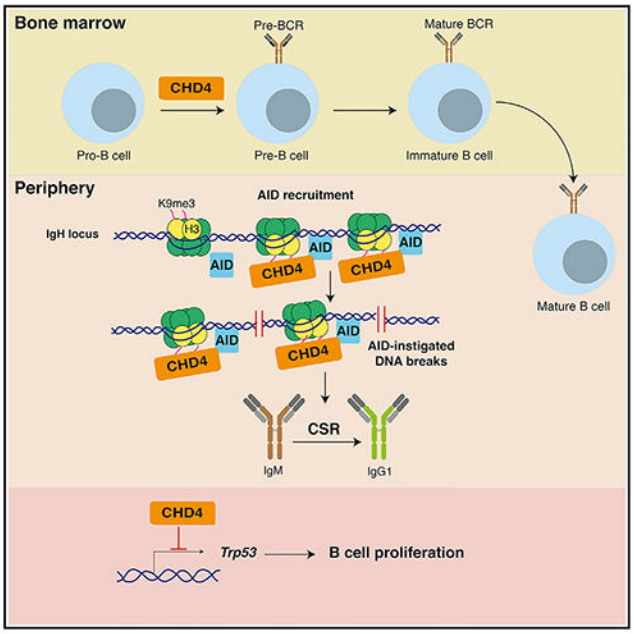

In Brief

Yen et al. demonstrate that CHD4, a component of the NuRD remodeling complex, is essential for early B cell development, represses p53 expression in mature B cells, and influences the recruitment of AID to DNA during class switch recombination.

INTRODUCTION

Because of the ability to produce and secrete antibodies against an almost infinite array of pathogens, B lymphocytes play a critical role in the adaptive immune response. Antibodies, or immunoglobulins (Igs), are composed of two heavy (Igh) and two light (Igκ or Igλ) chains covalently linked by disulfide bonds to form a tetrameric complex. The highly diverse N terminus variable regions of Igh and Igκ or Igλ contact antigens, while the less divergent C terminus constant region of Igh provides the effector function of the antibody molecule. The variable region exons of Igh and Igk or Igl are assembled in developing pro- and pre-B cells in the bone marrow from component variable (V), diversity(D), and joining (J) gene segments during the process of V(D)J recombination (Teng and Schatz, 2015). Upon exiting the bone marrow, the naive IgM^+ IgD^+ B cells migrate to secondary lymphoid organs (spleen, lymph nodes, Peyer's patches), where they encounter antigens and undergo *Igh* class switch recombination (CSR) and somatic hypermutation (SHM).

During SHM, which occurs primarily within microanatomical germinal center (GC) structures in lymphoid follicles, genes encoding the variable regions of Igh and Igκ or Igλ

are mutated at a very high rate (10^{-2} to 10^{-3}/bp/generation) to ultimately select B cells with higher antigen affinity (Mesin et al., 2016). CSR can occur within GCs or in the extra-follicular regions and exchanges the default Cμ constant region with one of a set of downstream constant region (C_h) gene segments (Cγ, Cε, Cα) (Xu et al., 2012; Yewdell and Chaudhuri, 2017). The B cell thereby changes from expressing IgM to one expressing IgG, IgE, or IgA, with each secondary isotype providing a distinct effector function during an immune response (Xu et al., 2012; Yewdell and Chaudhuri, 2017). Recent evidence strongly suggests that CSR also contributes to the generation of IgD-positive B cells from those expressing IgM (Chen and Cerutti, 2010; Rouaud et al., 2014).

CSR is a deletional-recombination reaction occurring between 1 and 12 kb long transcribed, repetitive switch (S) region DNA elements that precede each C_h gene segment (Alt et al., 2013; Xu et al., 2012; Yewdell and Chaudhuri, 2017). Prevailing models posit that activation induced cytidine deaminase (AID), a ~24 kDa protein essential for CSR, deaminates cytidines to uridines at transcribed S regions (Xu et al., 2012; Yewdell and Chaudhuri, 2017). Components of the general base-excision and mismatch repair pathways convert the deaminated residues into nicks and single-strand gaps that are ultimately processed into DNA double-strand breaks (DSBs). End-joining of DSBs between donor (usually Sμ) and acceptor S regions (Sγ, Sε,Sα) juxtaposes a new C_h gene downstream of the V(D)J segment and deletes the intervening DNA sequence as an extra-chromo- somal circle to complete the recombination reaction (Xu et al., 2012; Yewdell and Chaudhuri, 2017).

The mechanism by which AID is recruited to the *Igh* locus during CSR is intricately linked to germline transcription (Pavri, 2017; Yewdell and Chaudhuri, 2017). Each of the C_h genes is configured as individual germline transcription units composed of a cytokine- and activator-inducible promoter, an intervening I exon, an intronic S region, and C_h exons (Pavri, 2017; Yewdell and Chaudhuri, 2017). It is generally believed that transcription generates DNA structures, such as G quadruplexes and R loops, to facilitate AID recruitment and deamination (Chaudhuri et al., 2003; Duquette et al., 2005; Qiao et al., 2017; Yu and Lieber, 2003). Recent reports suggest that transcription also enables recruitment of AID to DNA via interaction with RNA polymerase II (Pol II), Spt5, RNA exosome machinery, PTBP2, and 14-3-3 adaptor proteins (Basu et al., 2011; Nowak et al., 2011; Pavri et al., 2010; Pefanis et al., 2014, 2015; Xu et al., 2010). Additionally, intronic segments of germline transcripts form G quadruplexes, bind AID, and have been implicated in recruiting AID to the *Igh* locus (Zheng et al., 2015). Thus, there is a generally broad understanding of trans-factors that facilitate recruitment of AID to its DNA substrates. However, what is largely unknown and remains a challenge is an understanding of how the chromatin landscape at the *Igh* locus interacts with and co-ordinates these various protein-DNA interactions to facilitate efficient AID targeting and CSR.

The N-terminal tails of the four core histones (H2A, H2B, H3, and H4) undergo extensive post-translational modifications (PTMs), including acetylation, phosphorylation, and methylation, to orchestrate the ordered recruitment of proteins that mediate DNA transactions (Tessarz and Kouzarides, 2014). The PTMs also attract factors that modulate chromatin structure via ATP-dependent nucleosome remodeling to alter chromatin accessibility. These combinatorial activities generate a permissive chromatin landscape for

factors required for replication, transcription, recombination, and repair (Tessarz and Kouzarides, 2014). The requirement for cell division, germline transcription, recruitment of specific DNA-modifying enzymes (AID), and long-range DSB repair suggests that CSR may use distinct PTMs to co-ordinate these myriad processes in a sequential and highly regulated manner within a clearly demarcated region of the B cell genome (Zan and Casali, 2015).

Consistent with this notion, S regions are hyper-accessible in activated B cells to DNA-modifying enzymes, with the accessibility pattern superimposable with histone PTMs that are generally associated with transcriptionally active chromatin (Wang et al., 2009). In naive unstimulated B cells, Sμ is enriched for activating histone marks including H3K4me3 (histone H3 trimethylated at lysine 4), H3K36me3, and H3K9acS10ph (H3K9ac9 phosphorylated serine 10). Upon B cell activation, these modifications spread to downstream S regions irrespective of their length (Wang et al., 2009). The functional relevance of the histone PTMs in CSR came from studies in which activities of the methyl transferases or acetyltransferases were altered and CSR was found to be perturbed. For example, depletion of Set1 or PTIP, proteins that promote H3K4me3, impaired CSR (Daniel et al., 2010; Stanlie et al., 2010). Likewise, loss of the histone acetyltransferases Pcaf and Gcn5 reduced H3K9AcS10ph at S regions and decreased CSR, mimicking CSR defect in B cells deleted for 14-3-3 adaptor proteins that interact with H3K9AcS10ph (Li et al., 2013). Because germline transcription is essential for CSR, it is plausible that the PTMs represent transcriptionally active chromatin at C_h genes engaged in CSR.

Intriguingly, S regions also accumulate H3K9me3 (histone H3 trimethylated at lysine-9), a mark correlated with inactive chromatin (Chowdhury et al., 2008; Jeevan-Raj et al., 2011; Kuang et al., 2009; Li et al., 2013; Wang et al., 2009). Additionally, over expression of Suv39h1, the methyltransferase that catalyzes methylation of H3K9, increased CSR while its loss impairs CSR to IgA (Bradley et al., 2006). H3K9me3 was initially linked to heterochromatin formation and gene silencing (Kouzarides, 2007). However, later studies revealed that H3K9me3 interacts with the chromo-domain containing heterochromatin protein 1γ (HP1γ) and that H3K9me3-HP1γ is present at actively transcribing genes and at recombining S regions (Bannister et al., 2001; Chowdhury et al., 2008; Jeevan-Raj et al., 2011; Kuang et al., 2009; Vakoc et al., 2005). Significantly, AID was detected in a complex with HP1g and KAP1 (KRAB domain associated protein-1), and deletion of KAP1 impaired CSR, leading to the proposal that the H3K9me3 serves to tether AID to S region DNA (Jeevan-Raj et al., 2011).

The chromo-domain-helicase-DNA binding protein 4, (CHD4, also referred to as Mi-2b) is a ~250 kDa protein that directly binds H3K9me3 through one of its PHD (plant homeodomain) fingers (Musselman et al., 2012). CHD4 also has a C terminus ATPase module, which uses energy from ATP hydrolysis to remodel nucleosomes. In this context, CHD4 is a component of the nucleosome remodeling and histone deacetylase (NuRD) complex, a large >2,000 kDa complex that also contains histone deacetylases (HDAC1 and HDAC2) and methyl-CpG-binding domain proteins (O'Shaughnessy and Hendrich, 2013). The dual properties of CHD4 that allow it to both recognize H3K9me3 and remodel chromatin via ATP hydrolysis suggest that it might participate in multiple aspects of

chromatin accessibility. Indeed, conditional inactivation of CHD4 in different lineages demonstrates its requirement at multiple stages of T cell development, including for normal expression of *CD4* (Williams et al., 2004), hematopoietic stem cell self-renewal (Yoshida et al., 2008), striated muscle identity (Gómez-Del Arco et al., 2016), and in the neural differentiation of embryonic stem cells (Hirota et al., 2019). Furthermore, short hairpin RNA (shRNA)- mediated depletion of CHD4 in a plasmacytoma cell line suggested that CHD4 negatively regulates expression of *Cd79a* in B cells (Ramírez and Hagman, 2009).

Because of the highly regulated role of transcription and chro- matin remodeling during CSR, as well as the presence of H3K9me3 at the *Igh* locus, CHD4 has the potential to serve as a critical epigenetic regulator of the process. However, despite the availability of conditionally deficient CHD4 (*Chd4*$^{fl/fl}$) mice (Williams et al., 2004), the requirement of CHD4 in B cells has not been investigated, likely because of pleiotropic effects and the impact on cell viability upon CHD4 loss. In this study, we conditionally knocked out *Chd4* at different stages of B cell development to demonstrate that CHD4 is essential for early B cell development, with a complete loss of the developing pre-B cell population. Strikingly, mature B cells tolerate the loss of CHD4, allowing us to investigate its role in CSR. Here, we demonstrate that CHD4 promotes proliferation of activated B cells in a p53-dependent manner. Furthermore, we show that CHD4 associates with the *Igh* locus, and its loss impairs CSR, potentially because of decreased AID targeting to S region DNA.

RESULTS

Depletion of CHD4 in *Ex Vivo* B Cell Cultures Impairs CSR

We first assessed if CHD4 is expressed in activated mature B cells. Naive splenic B cells were isolated from wild-type mice and stimulated in culture with LPS plus IL-4, a combination that promotes CSR to IgG1. CHD4 was detected in unstimulated B cells by western blotting, and there was no marked change in its expression following stimulation (Figure 1A). Likewise, when naive B cells were activated in culture to simulate a Th1 cytokine (IFN-γ plus LPS), or with an alternative T-dependent stimulation (anti-CD40 plus IL-21), no consistent alteration in CHD4 expression was observed (Figure S1).

To initially assess requirement of CHD4 in CSR, we retrovirally transduced shRNAs (Ramirez-Carrozzi et al., 2006) to deplete CHD4 in naive splenic B cells stimulated *ex vivo* with LPS plus IL-4 (Figure 1A). Knockdown of CHD4 led to a significant reduction in CSR to IgG1 compared with scrambled shRNA controls (Figure 1B). CHD4 depletion did not have any discernable effect on AID expression (Figure 1A) or B cell proliferation, as the total B cell numbers were unaltered (Figure 1C). To complement this approach, we retrovirally transduced cre recombinase into naive splenic B cells derived from *Chd4*$^{fl/fl}$ mice. Depletion of CHD4 protein (Figure 1D) was accompanied by a significant reduction in CSR to IgG1 (Figure 1E). There were no gross changes in AID expression (Figure 1D) or any marked effect on cell survival, as measured by the total number of live B cells at different time points post-stimulation (Figure 1F). Overall, results from these complementary strategies suggested that CHD4 influences CSR and provided the impetus to track B cell development and function *in vivo* upon stage-specific genetic deletion of CHD4.

CHD4 Is Essential for Early B Cell Development

To examine the requirement for CHD4 *in vivo*, we bred $Chd4^{fl/fl}$ mice to *Mb1-cre* mice, wherein the *Mb1* promoter drives cre expression. The *Mb1* gene encodes the Iga subunit of the B cell antigen receptor and is expressed in all B-lineage cells starting from the early pro-B cell stage. Thus, *Mb1-cre* mice are a convenient tool for B cell developmental studies (Hobeika et al., 2006). Relative to control mice, spleens of $Mb1^{cre/wt}Chd4^{fl/fl}$ mice were significantly smaller with reduced cellularity and had no detectable $B220^+$ $CD19^+$ mature B cells (Figure 2A). Examination of bone marrow of the $Mb1^{cre/wt}Chd4^{fl/fl}$ mice revealed a severe loss of $B220^+$ IgM^+ immature B cells and $B220^+$ IgM^+ recirculating B cells compared with controls (Figure 2B, top left), with a marked reduction in bone marrow cell numbers (Figure 2B). Further examination showed that $Mb1^{cre/wt}Chd4^{fl/fl}$ mice had a near complete loss of pre-B (IgM^- $B220^+$ $CD25^+$ $cKit^-$) cells and a marked increase in the frequency of pro-B (IgM^- $B220^+$ $CD25^-$ $cKit^+$) cells compared with control mice (Figure 2B). PCR genotyping confirmed that the loss of the floxed CHD4 allele in the bone marrow of the pro-B cells (Figure 2B, right). Thus, CHD4 is required for the development or maintenance of pre-B cells.

To examine if the loss of pre-B cells is due to the activation of a p53-dependent checkpoint associated with V(D)J recombina- tion (Gao et al., 2000; Guidos et al., 1996), we generated $Mb1^{cre/wt}Chd4^{fl/fl}p53^{fl/fl}$ mice. However, B cell development was not restored to any significant extent even after loss of p53 (Figure 2C). Transgenic expression of the anti-apoptotic Bcl-2 protein has been shown to restore early B cell lymphopoiesis in some instances (McDonnell et al., 1989), yet the Bcl-2 transgene could not restore B cell development in $Mb1^{cre/wt}Chd4^{fl/fl}$ mice (Figure 2D). Thus, CHD4 is essential for early B cell development, and its deletion leads to a severe loss of pre-B cells. However, the mechanism by which CHD4 participates in early B cell development is not currently well understood. Notably, this dramatic phenotype indicated that $Mb1^{cre/wt}Chd4^{fl/fl}$ mice could not serve as a productive model to study the function of CHD4 in mature B cells

Deletion of CHD4 in Mature B Cells Impairs CSR

To circumvent the early B cell developmental block, we tried deleting *Chd4* at a later stage of B cell development by breeding $Chd4^{fl/fl}$ mice to *Cd19-cre* mice. Unlike *Mb1-cre*, which results in the deletion of floxed alleles at the pro-B cell stage, *Cd19-cre* induces recombination at a later point, primarily during the pre-B stage (Rickert et al., 1997). The spleen of $Cd19^{cre/wt}Chd4^{fl/fl}$ mice (hereafter designated CHD4 knockout [KO]) had similar number and frequency of total splenocytes and $B220^+$ IgM^+ B cells as control mice, with no marked difference in spleen size (Figures 3A and S2A). Analysis of purified, naive splenic B cells from CHD4 KO mice showed efficient deletion of *Chd4* floxed alleles (Figure S2B) and loss of CHD4 protein (Figures 3B and S2C). Purified naive B cells from CHD4 KO and control mice were cultured *ex vivo* and stimulated with LPS plus IL-4 (Figure 3C) or anti-CD40 plus IL-4 (Figure S2C) to assess CSR to IgG1. CHD4 deficiency led to a severe defect in CSR, with CHD4 KO cells switching to IgG1 at only 25% of control cells (Figures 3C and S2C). Likewise, when naive splenic B cells were stimulated with LPS to evaluate CSR to IgG3, loss of CHD4 led to a similar reduction in IgG3 CSR as observed for IgG1 (Figure 3C).

In parallel with the above studies, we also generated *Cd21*^{cre}*Chd4*$^{fl/fl}$ mice wherein the *Cd21* promoter in a trans- gene drives cre expression starting from the IgM$^+$ IgD$^+$ mature B cells (Kraus et al., 2004). The splenic B220$^+$ IgM$^+$ B cell population was similar between *Cd21*^{cre}*Chd4*$^{fl/fl}$ mice and controls (Figure S2D). Consistent with data generated from *Cd19*$^{cre/wt}$*CHD4*$^{fl/fl}$ mice, B cells from *Cd21*^{cre}*Chd4*$^{fl/fl}$ also exhibited a severe defect in CSR to both IgG1 and IgG3 (Figure 3D). However, *Cd21*^{cre}*Chd4*$^{fl/fl}$ mice were born at non-Mendelian ratio (Figure S2E), likely because of non-specific deletion of CHD4 in the germline (Gostissa et al., 2013). We therefore used the *Cd19*$^{cre/wt}$*CHD4*$^{fl/fl}$ mice (CHD4 KO) for further analysis.

CHD4 Promotes Proliferation of B Cells in a p53- Dependent Manner

We sought to investigate potential molecular mechanisms by which CHD4 influences CSR. We observed that CHD4 deletion did not alter AID expression (Figures 3B and S2C) or germline transcription of activated C_h genes (Figure S3A). Annexin V staining demonstrated that stimulated CHD4 KO B cells did not exhibit increased apoptosis (Figure S3B). However, we observed markedly impaired proliferation of CHD4 KO splenic B cells as assessed by dilution of the tracking dye CFSE (Figure 4A). The defect in cell proliferation observed in CHD4 KO B cells was not observed upon CHD4 depletion by shRNA or cre recombinase (Figures 1C and 1F), likely because of residual CHD4 protein, which could not be detected within the sensitivity of the immunoblot.

To gain additional insights into CHD4 deficiency, we dissected its transcriptional network in splenic B cells undergoing CSR. We isolated RNA from purified splenic B cells stimulated with LPS and IL-4 stimulation for 48 h and performed RNA sequencing to identify candidate genes with distinct expression profiles upon CHD4 deletion. After focusing on more highly expressed transcripts (transcripts per million [TPM] > 10), our analysis identified 277 transcripts associated with 257 genes that were differentially expressed (DE; false discovery rate [FDR]-corrected p value < 0.05 and absolute $\log_2$ fold change > 0.5) (Figure 4B; Table S1). Among these genes, 133 had gene isoforms that were downregulated upon CHD4 deficiency, 120 had isoforms that were upregulated upon CHD4 deficiency, and 4 genes had isoforms that were either upregulated or downregulated. Gene set analysis among these DE genes showed enrichment of biological processes involved with lymphocyte activation, proliferation, and CSR (Figure 4C). For example, expression of CSR genes *Batf* and *Irf4*, two genes that positively regulate AID transcription, was increased, or decreased, respectively in CHD4 KO B cells (Ise et al., 2011; Sciammas et al., 2006). The differential effect of CHD4 loss on the expression of these two factors could explain why AID levels are unaltered in CHD4 KO B cells.

The most relevant data to emerge from this analysis are that several genes associated with proliferation were found to be DE (Figures 4B–4D). These included genes such as *Ccnd3*, *Ccl5*, *Fyn*, and notably *Trp53* (encoding p53 protein) (Figure 4D), with two *Trp53* isoforms, among the most significant DE transcripts (Figure 4B). Consistent with these transcript levels, we observed that p53 protein was also elevated in activated CHD4 KO splenic B cells (Figure 4E).

To investigate whether the impaired proliferation of CHD4 KO B cells was p53 dependent, we generated *Cd19*$^{cre/wt}$*Chd4*$^{fl/fl}$*p53*$^{fl/fl}$ mice (henceforth designated double KO [DKO] mice) to delete both p53 and CHD4 in B cells. Purified splenic B cells of all four genotypes (cre control, p53 KO, CHD4 KO, and DKO) were assayed for cell proliferation by CFSE dye dilution. Strikingly, p53 deficiency rescued the proliferation defect of CHD4 KO splenic B cells (Figure 4F). However, despite fully restoring the proliferative capacity of DKO B cells, p53 deletion was able to only mildly rescue CSR to IgG1 compared with controls (Figure 4G). On the basis of these results, we conclude that CHD4 influences CSR independent from its role in regulating cell proliferation via p53.

CHD4 Deletion Impairs GC Response and CSR *In Vivo*

To examine B cell responses *in vivo*, mice were immunized with sheep red blood cells (SRBC), a complex polyepitope T-dependent model system that induces a robust GC response in the spleen (Muramatsu et al., 2000). We observed that at day 14 (d14) post-immunization, total splenic B cell numbers were similar between control and CHD4 KO immunized mice (Figure 5A). As expected, SRBC immunization of control and AID KO mice led to a marked increase in the frequency of splenic GC (B220^{+} Fas^{+} GL7^{+}) B cells over mock PBS immunization (Figure 5B). However, CHD4 KO mice exhibited a severe reduction in the frequency of GC B cells compared with controls at d14 after SRBC immunization (Figure 5B). Additionally, the fraction of IgG1^{+} B cells among the GC B cell population was significantly reduced in immunized CHD4 KO mice relative to control animals (Figure 5C). Quantification of serum antibodies by ELISA revealed increased IgM levels upon SRBC immunization in both control and CHD4 KO mice (Figure 5D). However, increased IgG1 levels observed for control mice upon immunization was markedly suppressed in CHD4 KO B cells (Figure 5D), consistent with an immunization-dependent defect in CSR. Notably, deletion of p53 (in DKO mice) did not rescue the GC B cell response and *in vivo* IgG1 CSR defect to control (Figures 5B–5D). Overall, CHD4 deletion led to a severe defect in the GC B cell response to SRBC immunization.

To further characterize the *in vivo* B cell response, we used NP-CGG immunization, an extensively employed hapten T-dependent model antigen that facilitates identification of NP-specific B cells in the spleens of immunized mice (Jacob et al., 1991). Intracellular staining revealed that at d14 post-immunization, CHD4 protein was present at higher levels in GC B cells relative to naive B cells (Figure S4). In agreement with results obtained with SRBC immunization, CHD4 KO mice had markedly reduced frequency and absolute numbers of GC (B220^{+} GL7^{+} Fas^{+}) B cells (Figures 5E–5G and S5). Consistent with a CSR defect *in vivo*, we observed a marked reduction in the frequency of IgM^{-}IgD^{-}class-switched cells within the GC B cell population in CHD4 KO mice compared with control animals (Figure 5H). Thus, two different T-dependent immunization models demonstrated that CHD4 plays a critical role in the generation of GC B cells and in CSR *in vivo*.

The ability to track NP-specific B cells upon NP-CGG immunization allowed us to evaluate if CHD4 influences the emergence of early memory B cells, defined as splenic NP^{+} cells that are negative for the GC marker GL7 and express the surface marker CD38 (CD38^{+} GL7^{-}) (Figure S5) (Cho et al., 2016; Pucella et al., 2019). We found no significant

difference in the frequency of early memory B cells (NP^+ of $CD38^+$ $GL7^-$of $B220^+$ $CD19^+$) between control and CHD4 KO mice (Figure S6A). There was a slight increase in the average absolute number of early memory B cells; however, this difference was not statistically significant (Figure S6B). In contrast, the frequency of unswitched early memory B cells (IgM^+ of NP^+ $CD38^+$ $GL7^-$ $B220^+$) in CHD4 KO mice was increased (Figure S6C), while the frequency of class- switched early memory B cells (IgM^- IgD^- of NP^+ $CD38^+$ $GL7^-$ $B220^+$) was markedly reduced compared with control animals (Figure S6D), consistent with a CSR defect. Thus, it appears that loss of CHD4 does not have a major impact on the generation of antigen-specific early memory B cells, even though the frequency of switched cells among this population is significantly reduced. However, given the complex nature of B cell memory formation and its role in long-lived immunity, more exhaustive studies are required to elucidate the role of CHD4 in this process.

Whereas deletion of CHD4 led to a marked defect in CSR, the reduction in serum IgG1 levels in unimmunized mice was not as striking (Figure 5D). Likewise, at homeostasis, serum IgA levels (Figure S6E) or frequency of IgA^+ B cells in the GCs of Peyer's patches (Figures S6F and S6G) was similar between control and CHD4 KO mice. Thus, even though CHD4 KO B cells were intrinsically deficient for *in vitro* CSR to IgA (Figure S6H), conditions *in vivo* likely allow the selection and maintenance of the few cells that have managed to undergo CSR. This lack of correlation between *in vitro* and *in vivo* CSR is reminiscent of that observed for other CSR factors such as UNG and MSH2, wherein loss of either factor leads to a severe defect of CSR *in vitro* but has a much milder effect on homeostatic serum Ig levels *in vivo* (Rada et al., 2004).

Plasmablast Differentiation Is Not Grossly Affected by CHD4 Deletion

The differential requirement of CHD4 in different stages of B cell differentiation led us to explore if it has a role in plasmablast differentiation. Plasmablasts ($B220^{lo}$ $CD138^+$) represent an intermediate cell type that exhibits a transcriptional program very similar to that observed in plasma cells (Barwick et al., 2016). To assess plasmablast formation *ex vivo*, we activated naive B cells with LPS or LPS plus IL-4 for 96 h and assessed emergence of $B220^{lo}$ $CD138^+$ B cells (Barwick et al., 2016). We observed that CHD4 KO B cells were as proficient in generating plasmablasts as control B cells (Figures 6A and 6B). To assess the impact of CHD4 deletion on plasmablast differentiation *in vivo*, we used an intravenous immunization model with LPS, a T-independent sub-type 1 (TI-1) antigen that induces a rapid induction of $B220^{lo}$ $CD138^+$ plasmablasts in the spleen of immunized animals (Barwick et al., 2016; Pucella et al., 2019). As expected, we observed that relative to PBS-challenged (mock) mice, LPS administration induced robust plasmablast differentiation (Figure 6C). However, there was no difference in the frequency or absolute number of plasmablasts between control and CHD4 KO mice (Figures 6D and 6E). Intracellular staining showed that CHD4 protein expression was markedly diminished in the CHD4 KO plasmablasts (Figure 6F), indicating that the cells have not escaped cre-mediated CHD4 deletion. Thus, CHD4 is dispensable for formation of plasmablasts *ex vivo* and *in vivo*.

LPS administration also induces low levels of IgG3 CSR as a T-independent extra-follicular humoral response and a small fraction of the plasmablasts express IgG3; however,

intracellular staining showed that the frequency of $IgG3^+$ plasmablasts was similar between control and CHD4 KO mice (Figures 6G and 6H). Additionally, we did not detect any marked difference in the frequency of $B220^+$ $IgG3^+$ cells by surface staining between control and CHD4 KO mice (Figures 6J and 6K). However, both the $B220^{lo}$ $IgG3^+$ plasmablasts and the $B220^+$ $IgG3^+$ B cells still retained significant levels of CHD4 (Figures 6I and 6L). It is possible that LPS challenge induces a strong selection to generate $IgG3^+$ cells, and because only CHD4 sufficient cells are able to undergo efficient CSR, those cells that have escaped cre-mediated deletion are found in the $IgG3^+$ population. This could potentially explain the discrepancy in the requirement of CHD4 in inducing CSR in LPS-activated B cells *in vitro* (Figures 3C and 3D) versus LPS-challenged CSR *in vivo*.

CHD4 Promotes AID Recruitment

Our results have established the role of CHD4 in promoting the intrinsic ability of B cells to undergo CSR. With its well-docu- mented links with chromatin dynamics, it was logical to examine the possibility that CHD4 mediates CSR through a localized interaction with the *Igh* locus. To test this possibility, we first carried out chromatin immunoprecipitation (ChIP) experiments and observed that CHD4 was significantly enriched at Sm, but not at the control Cg1 region, in naive splenic B cells stimulated with LPS plus IL-4 (Figure 7A). The interaction of CHD4 with Sm was also observed in AID KO B cells (Figure 7A), suggesting that might be recruited upstream of DSBs, potentially through its ability to bind H3K9me3, an epigenetic mark implicated in AID targeting to donor Sm DNA (Chowdhury et al., 2008; Jee- van-Raj et al., 2011; Kuang et al., 2009; Li et al., 2013; Wang et al., 2009). In agreement with this notion, additional ChIP ex- periments demonstrated that H3K9me3 marks are enriched at Sm (Figure 7B). Interestingly, the H3K9me3 was present at Sm in-dependent of AID or CHD4 (Figure 7B), suggesting that this re- gion is poised to recruit factors that facilitate CSR.

To examine if CHD4 could bridge the interaction between AID and Sμ, we assessed the frequency of mutations at Sμ in LPS plus IL-4-activated splenic B cells. Mutations in Sμ are frequently observed in B cells activated in culture and serve as a surrogate for AID recruitment to DNA (Barreto et al., 2003; Schrader et al., 2003). In control B cells, the mutation frequency at this region was ~6.0×10^4/bp (Figures 7C and 7D). In contrast, the mutation frequency in CHD4 KO B cells was significantly reduced (~1.9×10^4/bp) (Figures 7C and 7D). Deletion of p53 in addition to CHD4 did not rescue the mutation frequency to control levels in the DKO cells (Figures 7C and 7D). Although higher than the mutation frequency (~0.25×10^4/bp) in AID-deficient B cells,the marked reduction in Sμ mutation frequency in CHD4 deficient B cells compared with controls strongly suggests a defect in AID recruitment to S region DNA.

To further test this hypothesis, we performed additional ChIP experiments to assess AID localization to Sm. At both 48 and 72 h post-stimulation with LPS+IL-4, CHD4 KO and DKO B cells had significantly reduced levels of AID bound to Sμ (Figures 7E, S7A, and S7C). Occupancy of AID at Cγ1 as a non- specific control region was at background level because the enrichment was similar to what was observed in AID KO B cells (Figure S7B), and there was no marked difference in the binding of H3 to Sμ in the different genotypes

examined (Figure S7C).Importantly, a reduction in both the frequency of Sμ mutations as well as AID occupancy at Sμ provides corroborative evidence that CHD4 influences the interaction of AID with *Igh* during CSR.

Finally, to test if CHD4 might interact with AID to mediate its recruitment to the *Igh* locus, we carried out co-immunoprecipitation experiments. We expressed FLAG-HA-tagged AID protein (2T-AID) along with a GFP reporter in AID KO splenic B cells via retroviral transduction (Figure 7F). We found that 2T-AID restored IgG1 switching in AID KO B cells (Figure 7G). When AID was immunoprecipitated from sorted GFP^+ B cells using HA antibodies, endogenous CHD4 was detected in the immune complex (Figure 7H). Although we could not detect an interaction between endogenous AID and CHD4, this result suggests that AID and CHD4 could form a protein complex in primary B cells, and this interaction could facilitate the optimal recruitment of AID to the *Igh* locus.

DISCUSSION

In this study, we used several genetic models to demonstrate that CHD4 is a versatile effector of B cell development and CSR. Deletion of CHD4 in pro-B cells leads to near-complete loss of the pre-B cell population. The severity of this defect could not be rescued by deletion of p53, suggesting that this phenotype is not likely due to cell cycle checkpoints associated with aberrant V(D)J recombination. Additionally, enforced expression of the anti-apoptotic gene Bcl-2 was unable to rescue pre-B cell development, indicating that CHD4 might not be influencing survival of developing pre-B cells. It is likely that CHD4 regulates expression of genes required for the pro-B to pre-B cell developmental transition, and the identity of such factors will require additional studies.

Remarkably, despite the absolute requirement of CHD4 in early B cell development, it is dispensable for homeostatic proliferation and survival of mature B cells. Loss of CHD4 in pre-B cells or mature B cells does not affect mature B cell numbers or survival. In response to T-dependent antigens, the formation of antigen-specific early memory B cells is not markedly impaired upon loss of CHD4, nor is the generation of plasmablasts in response to T-independent activators such as LPS. It is only under specific conditions of B cell activation such as CSR *in vitro* with different activators and cytokines, and CSR and GC formation *in vivo* in response to T-dependent antigens such as SRBC and NP-CGG, that the requirement of CHD4 is fully revealed. This context-dependent requirement of CHD4 at different stages of B cell development and function is reminiscent of its role in distinct stages of T cell development, including its requirement for expression of *CD4* but not *CD8* (Williams et al., 2004). The mechanism by which CHD4 participates in different cellular processes in a wide variety of cell types will require additional studies.

As a protein that responds to cellular stress including DSBs, p53 induces cell-cycle arrest and apoptosis and enforces genomic integrity in B cells from AID-induced genome-wide collateral damage during CSR (Robbiani et al., 2009; Zilfou and Lowe, 2009). However, p53 activity must be downregulated for B cell survival and proliferation in the face of ongoing *Igh* DSBs during CSR (Phan and Dalla-Favera, 2004). Our results clearly demonstrate that CHD4 represses p53 mRNA expression to promote B cell proliferation. Regulation of p53

expression likely rep- resents the role of CHD4 as an essential component of the NuRD transcriptional repressor complex. The NuRD complex also contains the HDAC1/2 deacetylases, which could also influence p53 stability via regulating its acetylation (Hirota et al., 2019; Polo et al., 2010). Whether both transcriptional and post-transcriptional activities of the NuRD complex contribute to regulate p53 levels in activated B cells is not clear at present, but both appear to be mediated via NuRD-dependent function of CHD4. In this regard, another NuRD complex associated factor ZMNYD8 has recently been shown to influence CSR by regulating the activity of the 3′Igh super-enhancer (Delgado-Benito et al., 2018). Additionally, on the basis of the ability of the NuRD complex to regulate acetylation of p53 protein, it is possible that it could also impact PTMs of AID and other factors that participate in different stages of B cell development and differentiation.

Our results provide clear evidence that CHD4 influences the recruitment of AID to *Igh*. One possible mechanism for CHD4- mediated AID targeting is through the ability of CHD4 to directly bind H3K9me3, a histone PTM enriched at S regions (Chowd- hury et al., 2008; Jeevan-Raj et al., 2011; Kuang et al., 2009; Li et al., 2013; Wang et al., 2009). Although generally associated with transcriptionally repressed chromatin states, H3K9me3 mark has been found on some transcribed genes (Vakoc et al., 2005) and has also been implicated in establishing an environment permissive to long-range chromosomal interactions (Jee- van-Raj et al., 2011; Jia et al., 2004). In this regard, AID interacts with the KRAB domain-associated protein 1 (KAP1):heterochromatin protein 1 (HP1) complex that is tethered to H3K9me3 at the *Igh* locus (Jeevan-Raj et al., 2011), and CHD4 has been implicated in the recruitment of KAP1-HP1 to H3K9me3-marked chromatin (Price and D'Andrea, 2013). Therefore, it is quite possible that CHD4 facilitates recruitment of AID to DNA by targeting a KAP1-HP1-AID complex to H3K9me3 at S regions during CSR. Such a mechanism, wherein only a subset of transcriptionally active genes retains the H3K9me3 mark, could potentially explain how AID is targeted to a relatively limited number of transcribed genes in B cells.

CHD4 has been shown to participate in the repair of DNA DSBs (O'Shaughnessy and Hendrich, 2013). It is recruited to sites of DNA damage and, as a chromatin remodeler, could generate an environment permissive to amplification of the DNA-damage response and recruitment of factors required for DNA repair (O'Shaughnessy and Hendrich, 2013). Whether CHD4 influences DSB repair during CSR is yet to be determined. However, the observations that both KAP-1 and CHD4 participate in DNA damage response in an ATM-dependent manner (Urquhart et al., 2011; Ziv et al., 2006) is consistent with a general theme (Vuong et al., 2013) that CSR proceeds in a highly coordinated reaction wherein the factors that promote DSB formation at the *Igh* locus also promote repair, providing one mechanism by which genomic integrity can be maintained in B cells in the face of deliberate DNA damage.

In summary, we have identified CHD4 as a stage-specific effector of B cell development and differentiation. We have demonstrated that CHD4 influences the formation of GC B cells upon immunization with T-dependent antigens and plays a critical role in B cell proliferation in a p53-dependent fashion. Finally, we have established that CHD4 influences the recruitment of AID to the *Igh* locus during CSR. These results lead to new outstanding

questions regarding the distinct roles of CHD4 across multiple facets of B cell biology and how epigenetic modifications specify AID recruitment in a CHD4-specific manner to the *Igh* locus, potentially sheltering the rest of the genome from AID-induced destabilization during CSR.

STAR★METHODS

CONTACT FOR REAGENT AND RESOURCE SHARING

Further information and requests for resources and reagents should be directed to and will be fulfilled by the Lead Contact, Jayanta Chaudhuri (chaudhuj@mskcc.org).

EXPERIMENTAL MODEL AND SUBJECT DETAILS

Aicda$^{-/-}$ (Muramatsu et al., 2000), *Mb1*$^{cre/cre}$ (Hobeika et al., 2006) and *Vav-Bcl2* (Egle et al., 2004) mice were respectively, kindly provided by Tasuku Honjo (University of Kyoto, Japan), Alexander Tarakhovsky (Rockefeller University, USA) and Ari Melnick (Weill Cornell Medical School). *Aicda*$^{cre/cre}$ mice (Robbiani et al., 2008) were obtained from the Nussenzweig lab (Rockefeller University,USA). Generation of *Chd4*$^{fl/fl}$ mice was described previously (Williams et al., 2004). *Cd19*$^{cre/cre}$, *Cd21*^{cre}, *p53*$^{fl/fl}$ and C57BL/6J were purchased from the Jackson Laboratories (Bar Harbor, ME). 8–16 week old mice of both sexes were used and whenever possible littermates were used as controls. Mice used in the experiments were maintained in specific pathogen free conditions in Memorial Sloan Kettering Cancer Center vivarium according to the institutional guidelines.

METHOD DETAILS

Purified B cell cultures—Splenic B cells from naive mouse were purified by anti-CD43 negative selection according to manufacturer's protocol (Miltenyi Biotec #130-049-801). Purified B cells were cultured in B cell media as described earlier (Pucella et al., 2019). Naive B cells were stimulated with LPS (30 μg/ml, Sigma, #L4130) for IgG3 CSR and LPS plus mouse IL-4 (12.5ng/ml, R&D Systems) or anti-CD40 (10ng/ml, eBioscience clone HM40–3, #16–0402) plus IL-4 (12.5 ng/ml) for CSR to IgG1. For IgA CSR, B cells were cultured with LPS (5μg/mL), BAFF (20ng/mL), IL-4 (10ng/mL), IL-5 (10ng/mL), TGF-β (10ng/mL) and Retinoic acid (10nM). Naive B cells were also cultured in LPS(10 μg/ml) plus mouse IFN-γ (50ng/ml, Gemini Bio-products, #300–311P) or mouse anti-CD40 (10ng/ml) plus IL-21 (50ng/ml, R&D systems). Usually, B cells cultures were initiated at 0.5–1.0×10^6/ml and diluted 1:2 at 48h and 72h and analyzed for CSR at 96h.

Retroviral infection—Short hairpin RNAs against mouse CHD4 (5'-GACTACGACCTGTTCAAGCAG-3') or scrambled (5'-GCGAAAGATGATAAGCTAA-3') was obtained from Addgene (plasmid 15379). MSCV-cre was obtained from Addgene (plasmid 24064). Retroviral transduction of splenic B cells has been described earlier (Drané et al., 2017). Briefly, retrovirus supernatant was prepared by co-transfecting pMIG, 2T-AID, or CHD4 shRNA plasmids with packaging vector pCL-Eco into HEK293T cells using calcium phosphate. Purified splenic B cells (2×10^6) were plated at a density of 1–2 × 10^6 cells per/ml and stimulated with 30 mg/ml LPS plus 12.5 ng/ml IL-4. After stimulation for 24 h and 48 h, media were aspirated, leaving approximately 1 ml of media per well of a six-

well dish, and retroviruses were added. Six-well dishes were spun at 2,000 *g* for 90 min at 32°C, after which viral supernatants were aspirated and fresh B cell media plus LPS and IL-4 was added. Cells were analyzed 48h after the second round of infection.

Flow cytometry and sorting—For flow cytometeric analysis, cells were washed with FACS buffer (1 × PBS, 2.5% FBS), resuspended in 100 μl FACS buffer, incubated with an Fc blocking reagent (BD PharMingen) and stained at 4°C with antibodies to various cell surface antigens. Viability was assessed with DAPI (Invitrogen) or Zombie red fixable (BioLegend). Cells were washed 1× with FACS buffer, and resuspended in 200 μl FACS buffer. Flow cytometric analysis of CFSE or Annexin V stainings was performed according to manufacturer's instructions (CellTrace CFSE Cell Proliferation Kit, Invitrogen and FITC Annexin V Apoptosis Detection Kit, BD Biosciences. Briefly, purified naive B cells were stained with 5 μM CFSE and cultured for 96 h in LPS plus IL-4 and CFSE dilution was monitored by flow cytometer. GFP^+ cells or bone marrow B cell populations were sorted in a FACSAria cell sorter (BD Biosciences). Flow cytometry was performed using an LSR-II flow cytometer (BD Biosciences), and data analyzed using FlowJo software (version 9.9).

Immunization—Mice were intra-peritoneally injected with 1×10^8 packed sheep red blood cells in 200 μl of PBS (Innovative Research #IC10-0210) on day 0, followed by a boost of the same number of packed cells on day 10. The spleens of immunized or PBS mock-injected control mice were analyzed on day 14. For NP-CGG immunization, NP(31)-CGG (no. N-5055D-5; Biosearch Technologies) was precipitated with Imject alum adjuvant (no. 77161; Thermo Fisher Scientific). Mice were immunized intra-peritoneally in 100 μl doses with 50 μg on day 0 and boosted with 50 μg NP-CGG in alum on day 10. B cells in the spleens of immunized or PBS-injected mice were analyzed d14. For LPS challenge, TLRgrade LPS from *Salmonella minnesota* R595 (no. ALX-581–008- L002) was purchased from Enzo Life Sciences. Mice were immunized intravenously with 50 μg LPS in sterile PBS (100 μl) on d0 and sacrificed on d5 to assess plasmablast formation.

Sμ mutation analysis—The 5′ end of Sμ was amplified by PCR using Phusion High-Fidelity DNA Polymerase (NEB) with primers SmF (5′-AATGGATACCTCAGTGGTTTTTAATGGTGGGTTTA-3′) and SmR (5′-GCGGCCCGGCTCATTCCAGTTCATTACAG-3′) as described previously (Barreto et al., 2003). The PCR amplification conditions were as follows: 30 cycles of 94°C (15 s), 60° C (15 s), and 68° C (1 min).PCR products were cloned into TOPO PCR Cloning vector (Invitrogen) and then sequenced (GENEWIZ). Sequences were aligned with Lasergene (DNASTAR) and analyzed for mutational frequencies.

Protein analysis—Protein extracts from primary B cell cultures or sorted GFP^+ splenic B cells were prepared using NP-40 lysis buffer (20 mM Tris-Cl, pH8.0, 150–650 mM mM NaCl, 1 mM EDTA, 0.5% NP-40) plus protease inhibitors (cOmplete Mini, EDTA-free Roche Cat#11836170001). For immunoprecipitation, lysates were centrifuged at 15,000 × *g* for 20 min, and the supernatant was collected as cell-free extracts. Extracts (0.5 mg) were precleared with agarose beads and then incubated with anti-HA agarose (Pierce) at 4°C overnight and subsequently with protein A agarose beads for another 90 min. The

immunoprecipitate was washed twice with low-salt buffer (150 mM NaCl), once with high-salt buffer (500 mM NaCl), and then with 1 × Tris-buffered saline. The proteins were eluted with 2 × SDS sample loading buffer, and analyzed by immunoblotting. The AID antibody used in this study was described earlier (Chaudhuri et al., 2003).

Chromatin immunoprecipitation—Splenic B cells from 8–10 week old mice were isolated and ChIP was performed according to protocol described in the ChIP Assay Kit (Millipore, 17–295). Briefly, splenic B cells were stimulated with LPS (30 μg/ml) plus mouse IL-4 (12.5ng/ml) for 48h or 72h. Approximately 1.0×10^7 activated cells were cross-linked by adding fresh 11% formaldehyde to a final concentration of 1% and incubating at room temperature for 10 minutes. The reaction was neutralized by adding 1:20 volumes of 2.5M glycine (pH 8.0). Cross-linked cells were washed with PBS-based Cell Wash Buffer (PBS, 0.1% FBS, 2mM EDTA) and lysed according to the protocol of truChIP Chromatin Shearing Kit with Formaldehyde (Covaris, 520154). Cell lysates were sonicated in the M220 Focused-ultrasonicator (Covaris, 5002295) to shear the chromatin, and debris was removed by centrifugation. Sonicated lysates were diluted to 1.5 mL in ChIP dilution buffer and pre-cleared according to manufacturer's protocol. Pre-cleared lysate was divided into three parts of 500 μL each and incubated with 1 μg of anti-H3 antibody (Abcam), 2 μg of anti-AID antibody (Chaudhuri et al., 2003) or control IgG (Jackson Immunoresearch Labs) at 4˚C overnight. Immunocomplexes were recovered with salmon sperm DNA/Protein A agarose slurry and washed with the sequence of buffers listed in the protocol (1ml per wash). Immuno complexes were eluted from the beads using 500 μL of fresh elution buffer (1% SDS and 0.1M $NaHCO_3$) and cross-linking was reversed by incubation with 5M NaCl (final concentration 0.3M) and RNase A (30 μg/ml) at 65˚C for 4–6h. The samples were then treated with 20 μL of 1M Tris pH 6.5, 10 mL of 0.5M EDTA and 2 μL proteinase K (10mg/ml) for 1 hour at 45˚C. DNA was recovered by phenol-chloroform extraction and ethanol precipitation with carrier glycogen. Pellets were resuspended in 35 μL of water for use as ChIP DNA or 50 μL of water for use as input DNA. DNA was analyzed by qPCR using PowerUp SYBR Green Master Mix (Applied Biosystems) for Sm and negative control locus Cγ1.

ELISA

Coating antibodies for binding IgA, IgM and IgG1 were purchased from Southern Biotechnology Associates (key resources table). Isotype standards used to calculate absolute concentration values are listed in the key resources table. HRP-labeled secondary antibodies for detecting IgA, IgM and IgG1 were purchased are listed in the key resources table. eBioscience ELISA diluent (no. 00-4202-56) was used as blocking buffer, TMB substrate (no. 00-4201-56) was used to develop, and 1 M phosphoric acid was used to stop development. Plates were read at 450 nm on a BioTek Synergy HT detector. Absolute concentrations of serum Abs were determined by interpolation from the standard curve, with attention paid to keeping values within standard and sample linear ranges. All samples were analyzed in duplicate over an eight-step dilution series.

RNA sequencing and analysis—Splenic B cells were isolated and stimulated with LPS plus IL-4 for 48h. RNA was isolated using TRIzol (Invitrogen) and RNeasy Mini Kit

(QIAGEN catalog # 74104) according to instructions provided by the manufacturer. After RiboGreen quantification and quality control by Agilent BioAnalyzer, 2 ng total RNA with RNA integrity numbers ranging from 8.1 to 9.6 underwent amplification using the SMART-Seq v4 Ultra Low Input RNA Kit (Clontech catalog # 63488), with 12 cycles of amplification. Subsequently, 10 ng of amplified cDNA was used to prepare libraries with the KAPA Hyper Prep Kit (Kapa Biosystems KK8504) using 8 cycles of PCR. Samples were barcoded and run on a HiSeq 4000 in a 50bp/50bp paired end run, using the HiSeq 3000/4000 SBS Kit (Illumina). An average of 56.8 million paired reads were generated per sample and the percent of mRNA bases per sample ranged from 58% to 75%.

Paired-end reads were trimmed for adaptors and removal of low quality reads using Trimmomatic (v.0.36) (Bolger et al., 2014).Transcript quantification was based on the mm10 UCSC Known Gene models and performed using the quasi-mapping-based mode of Salmon (v.0.8.2) (Patro et al., 2017), correcting for potential GC base pair bias. Differential analyses were performed on the transcript level using tximport (v.1.8.0) (Soneson et al., 2015) and DESeq2 (v1.14.1) (Love et al., 2014). Transcripts were considered differentially expressed (DE) if they showed a false discovery rate (FDR)-adjusted P value < 0.05, an absolute log2 fold change of 0.5, and an average transcripts-per-million (TPM, calculated by Salmon) > 10.

Gene set analysis was performed using GOseq (v.1.26.0) (Young et al., 2010), using gene IDs from DE transcripts, and the “bio-logical process” subgroup of gene sets curated by the Gene Ontology Consortium (Ashburner et al., 2000). Transcripts that weremissing gene IDs as designated by UCSC were assigned Entrez IDs based on gene name using the org.Mm.eg.db R package(v.3.4.0) before performing gene set analysis. Transcripts that had no ID assigned were dropped. FDR-corrected P values were calculated from P values calculated by GOseq, and only gene ontologies passing a threshold of $p < 0.05$ and contained at least 10 DE genes were considered. Top 10 gene sets that contained the highest proportion of DE genes out of the total gene set are depicted. The gene set titled, “adaptive immune response based on somatic recombination of immune receptors built from immunoglobulin superfamily domains” was renamed to “CSR genes.”

QUANTIFICATION AND STATISTICAL ANALYSIS

All statistical analyses were performed using Prism (GraphPad). Graphs represent data from at least 2 independent experiments, each consisting of at least 3 biological replicates. The exact number of the biological replicates (*n*) in the presented dataset is indicated in the figure legends. Results are expressed as mean ± SD. Two-tailed, unpaired Student’s t test was performed on individual biological replicates. Differences were considered significant when *P value*s were < 0.05. *P value*s > 0.05 are either not shown or marked with n.s. (not significant), *p < 0.05, **p < 0.005.

DATA AND SOFTWARE AVAILABILITY

RNA-seq data have been deposited in the Gene Expression Omnibus under accession number GEO: GSE128321.

Supplementary Material

Refer to Web version on PubMed Central for supplementary material.

ACKNOWLEDGMENTS

We are extremely grateful to Katia Georgopoulos, Massachusetts General Hospital, for providing us with the *CHD4*$^{fl/fl}$ mice. We would like to thank members of the Chaudhuri, Rudensky, and Koralov labs for technical assistance and discussion; A. Bravo for help with maintenance of the mouse colony; and Wei Hu for immunoblot advice. J.C. was supported by grants from the NIH (1RO1AI072194, 1RO1AI124186, and P30CA008748), the Starr Cancer Research Foundation, the Ludwig Cancer Center, MSKCC Functional Genomics, and the Geoffrey Beene Cancer Center. A.Y.R. was supported by NIH grants R37 AI034206 and P30CA008748, as well as the Hilton-Ludwig Cancer Prevention Initiative funded by the Conrad N. Hilton Foundation and Ludwig Cancer Research. A.Y.R. is an investigator with the Howard Hughes Medical Institute. C.M.L. was supported by a T32 award from the NIH (CA009149) and is a Cancer Research Institute-Carson Family Fellow. W.T.Y. was supported by a Special Fellow award from the Leukemia & Lymphoma Society and a NIH T32 training grant (CA009149). J.C.S. was supported by the Ludwig Center for Cancer Immunotherapy, the Burroughs Wellcome Fund, the American Cancer Society, and grants from the NIH (AI100874, AI130043, and P30CA008748). S.B.K. was supported by grants from the NIH (R21AI137752) and the Binational Science Foundation. We acknowledge the use of the MSKCC Integrated Genomics Operation Core, funded by the NCI Cancer Center Support Grant (CCSG; P30 CA08748), Cycle for Survival, and the Marie-Josée and Henry R. Kravis Center for Molecular Oncology.

REFERENCES

Alt FW, Zhang Y, Meng FL, Guo C, and Schwer B (2013). Mechanisms of programmed DNA lesions and genomic instability in the immune system. Cell 152, 417–429. [PubMed: 23374339]

Ashburner M, Ball CA, Blake JA, Botstein D, Butler H, Cherry JM, Davis AP, Dolinski K, Dwight SS, Eppig JT, et al.; The Gene Ontology Consortium (2000). Gene Ontology: tool for the unification of biology. Nat. Genet 25, 25–29. [PubMed: 10802651]

Bannister AJ, Zegerman P, Partridge JF, Miska EA, Thomas JO, Allhire RC, and Kouzarides T (2001). Selective recognition of methylated lysine 9 on histone H3 by the HP1 chromo domain. Nature 410, 120–124. [PubMed: 11242054]

Barreto V, Reina-San-Martin B, Ramiro AR, McBride KM, and Nussenzweig MC (2003). C-terminal deletion of AID uncouples class switch recombination from somatic hypermutation and gene conversion. Mol. Cell 12, 501–508. [PubMed: 14536088]

Barwick BG, Scharer CD, Bally APR, and Boss JM (2016). Plasma cell differentiation is coupled to division-dependent DNA hypomethylation and gene regulation. Nat. Immunol 17, 1216–1225. [PubMed: 27500631]

Basu U, Meng FL, Keim C, Grinstein V, Pefanis E, Eccleston J, Zhang T, Myers D, Wasserman CR, Wesemann DR, et al. (2011). The RNA exosome targets the AID cytidine deaminase to both strands of transcribed duplex DNA substrates. Cell 144, 353–363. [PubMed: 21255825]

Bolger AM, Lohse M, and Usadel B (2014). Trimmomatic: a flexible trimmer for Illumina sequence data. Bioinformatics 30, 2114–2120. [PubMed: 24695404]

Bradley SP, Kaminski DA, Peters AH, Jenuwein T, and Stavnezer J (2006). The histone methyltransferase Suv39h1 increases class switch recombination specifically to IgA. J. Immunol 177, 1179–1188. [PubMed: 16818776]

Chaudhuri J, Tian M, Khuong C, Chua K, Pinaud E, and Alt FW (2003). Transcription-targeted DNA deamination by the AID antibody diversification enzyme. Nature 422, 726–730. [PubMed: 12692563]

Chen K, and Cerutti A (2010). New insights into the enigma of immunoglobulin D. Immunol. Rev 237, 160–179. [PubMed: 20727035]

Cho SH, Raybuck AL, Stengel K, Wei M, Beck TC, Volanakis E, Thomas JW, Hiebert S, Haase VH, and Boothby MR (2016). Germinal centre hypoxia and regulation of antibody qualities by a hypoxia response system. Nature 537, 234–238. [PubMed: 27501247]

Chowdhury M, Forouhi O, Dayal S, McCloskey N, Gould HJ, Felsenfeld G, and Fear DJ (2008). Analysis of intergenic transcription and histone modification across the human immunoglobulin heavy-chain locus. Proc. Natl. Acad. Sci. U S A 105, 15872–15877. [PubMed: 18836073]

Daniel JA, Santos MA, Wang Z, Zang C, Schwab KR, Jankovic M, Filsuf D, Chen HT, Gazumyan A, Yamane A, et al. (2010). PTIP promotes chromatin changes critical for immunoglobulin class switch recombination. Science 329, 917–923. [PubMed: 20671152]

Delgado-Benito V, Rosen DB, Wang Q, Gazumyan A, Pai JA, Oliveira TY, Sundaravinayagam D, Zhang W, Andreani M, Keller L, et al. (2018). The chromatin reader ZMYND8 regulates Igh enhancers to promote immunoglobulin class switch recombination. Mol. Cell 72, 636–649.e8. [PubMed: 30293785]

Drané P, Brault ME, Cui G, Meghani K, Chaubey S, Detappe A, Parnandi N, He Y, Zheng XF, Botuyan MV, et al. (2017). TIRR regulates 53BP1 by masking its histone methyllysine binding function. Nature 543, 211–216. [PubMed: 28241136]

Duquette ML, Pham P, Goodman MF, and Maizels N (2005). AID binds to transcription-induced structures in c-MYC that map to regions associated with translocation and hypermutation. Oncogene 24, 5791–5798. [PubMed: 15940261]

Egle A, Harris AW, Bath ML, O'Reilly L, and Cory S (2004). VavP-Bcl2 transgenic mice develop follicular lymphoma preceded by germinal center hyperplasia. Blood 103, 2276–2283. [PubMed: 14630790]

Gao Y, Ferguson DO, Xie W, Manis JP, Sekiguchi J, Frank KM, Chaudhuri J, Horner J, DePinho RA, and Alt FW (2000). Interplay of p53 and DNA-repair protein XRCC4 in tumorigenesis, genomic stability and development. Nature 404, 897–900. [PubMed: 10786799]

Gómez-Del Arco P, Perdiguero E, Yunes-Leites PS, Acín-Pérez R, Zeini M, Garcia-Gomez A, Sreenivasan K, Jiménez-Alcázar M, Segalés J, Ló- pez-Maderuelo D, et al. (2016). The chromatin remodeling complex Chd4/NuRD controls striated muscle identity and metabolic homeostasis. Cell Metab 23, 881–892. [PubMed: 27166947]

Gostissa M, Bianco JM, Malkin DJ, Kutok JL, Rodig SJ, Morse HC 3rd, Bassing CH, and Alt FW (2013). Conditional inactivation of p53 in mature B cells promotes generation of nongerminal center-derived B-cell lymphomas. Proc. Natl. Acad. Sci. U S A 110, 2934–2939. [PubMed: 23382223]

Guidos CJ, Williams CJ, Grandal I, Knowles G, Huang MT, and Danska JS (1996). V(D)J recombination activates a p53-dependent DNA damage checkpoint in scid lymphocyte precursors. Genes Dev 10, 2038–2054. [PubMed: 8769647]

Hirota A, Nakajima-Koyama M, Ashida Y, and Nishida E (2019). The nucleosome remodeling and deacetylase complex protein CHD4 regulates neural differentiation of mouse embryonic stem cells by down-regulating p53. J. Biol. Chem 294, 195–209. [PubMed: 30409903]

Hobeika E, Thiemann S, Storch B, Jumaa H, Nielsen PJ, Pelanda R, and Reth M (2006). Testing gene function early in the B cell lineage in mb1-cre mice. Proc. Natl. Acad. Sci. U S A 103, 13789–13794. [PubMed: 16940357]

Ise W, Kohyama M, Schraml BU, Zhang T, Schwer B, Basu U, Alt FW, Tang J, Oltz EM, Murphy TL, and Murphy KM (2011). The transcription factor BATF controls the global regulators of class-switch recombination in both B cells and T cells. Nat. Immunol 12, 536–543. [PubMed: 21572431]

Jacob J, Kassir R, and Kelsoe G (1991). In situ studies of the primary immune response to (4-hydroxy-3-nitrophenyl)acetyl. I. The architecture and dynamics of responding cell populations. J. Exp. Med 173, 1165–1175. [PubMed: 1902502]

Jeevan-Raj BP, Robert I, Heyer V, Page A, Wang JH, Cammas F, Alt FW, Losson R, and Reina-San-Martin B (2011). Epigenetic tethering of AID to the donor switch region during immunoglobulin class switch recombination.J. Exp. Med 208, 1649–1660. [PubMed: 21746811]

Jia S, Yamada T, and Grewal SI (2004). Heterochromatin regulates cell type-specific long-range chromatin interactions essential for directed recombination. Cell 119, 469–480. [PubMed: 15537537]

Kouzarides T (2007). Chromatin modifications and their function. Cell 128, 693–705. [PubMed: 17320507]

Kraus M, Alimzhanov MB, Rajewsky N, and Rajewsky K (2004). Survival of resting mature B lymphocytes depends on BCR signaling via the Igalpha/beta heterodimer. Cell 117, 787–800. [PubMed: 15186779]

Kuang FL, Luo Z, and Scharff MD (2009). H3 trimethyl K9 and H3 acetyl K9 chromatin modifications are associated with class switch recombination. Proc. Natl. Acad. Sci. U S A 106, 5288–5293. [PubMed: 19276123]

Li G, White CA, Lam T, Pone EJ, Tran DC, Hayama KL, Zan H, Xu Z, and Casali P (2013). Combinatorial H3K9acS10ph histone modification in IgH locus S regions targets 14-3-3 adaptors and AID to specify antibody class- switch DNA recombination. Cell Rep 5, 702–714. [PubMed: 24209747]

Love MI, Huber W, and Anders S (2014). Moderated estimation of fold change and dispersion for RNA-seq data with DESeq2. Genome Biol 15, 550. [PubMed: 25516281]

McDonnell TJ, Deane N, Platt FM, Nunez G, Jaeger U, McKearn JP, and Korsmeyer SJ (1989). bcl-2-immunoglobulin transgenic mice demon strate extended B cell survival and follicular lymphoproliferation. Cell 57, 79–88. [PubMed: 2649247]

Mesin L, Ersching J, and Victora GD (2016). Germinal center B cell dynamics. Immunity 45, 471–482. [PubMed: 27653600]

Muramatsu M, Kinoshita K, Fagarasan S, Yamada S, Shinkai Y, and Honjo T (2000). Class switch recombination and hypermutation require activation-induced cytidine deaminase (AID), a potential RNA editing enzyme. Cell 102, 553–563. [PubMed: 11007474]

Musselman CA, Ramírez J, Sims JK, Mansfield RE, Oliver SS, Denu JM, Mackay JP, Wade PA, Hagman J, and Kutateladze TG (2012). Bivalent recognition of nucleosomes by the tandem PHD fingers of the CHD4 ATPase is required for CHD4-mediated repression. Proc. Natl. Acad. Sci. U S A 109, 787–792. [PubMed: 22215588]

Nowak U, Matthews AJ, Zheng S, and Chaudhuri J (2011). The splicing regulator PTBP2 interacts with the cytidine deaminase AID and promotes binding of AID to switch-region DNA. Nat. Immunol 12, 160–166. [PubMed: 21186367]

O'Shaughnessy A, and Hendrich B (2013). CHD4 in the DNA-damage response and cell cycle progression: not so NuRDy now. Biochem. Soc. Trans 41, 777–782. [PubMed: 23697937]

Patro R, Duggal G, Love MI, Irizarry RA, and Kingsford C (2017). Salmon provides fast and bias-aware quantification of transcript expression. Nat. Methods 14, 417–419. [PubMed: 28263959]

Pavri R (2017). R loops in the regulation of antibody gene diversification. Genes (Basel) 8, E154. [PubMed: 28574479]

Pavri R, Gazumyan A, Jankovic M, Di Virgilio M, Klein I, Ansarah-So- brinho C, Resch W, Yamane A, Reina San-Martin B, Barreto V, et al. (2010). Activation-induced cytidine deaminase targets DNA at sites of RNA po- lymerase II stalling by interaction with Spt5. Cell 143, 122–133. [PubMed: 20887897]

Pefanis E, Wang J, Rothschild G, Lim J, Chao J, Rabadan R, Econo- mides AN, and Basu U (2014). Noncoding RNA transcription targets AID to divergently transcribed loci in B cells. Nature 514, 389–393. [PubMed: 25119026]

Pefanis E, Wang J, Rothschild G, Lim J, Kazadi D, Sun J, Federation A, Chao J, Elliott O, Liu ZP, et al. (2015). RNA exosome-regulated long non-coding RNA transcription controls super-enhancer activity. Cell 161, 774–789. [PubMed: 25957685]

Phan RT, and Dalla-Favera R (2004). The BCL6 proto-oncogene sup- presses p53 expression in germinal-centre B cells. Nature 432, 635–639. [PubMed: 15577913]

Polo SE, Kaidi A, Baskcomb L, Galanty Y, and Jackson SP (2010). Regulation of DNA-damage responses and cell-cycle progression by the chromatin remodelling factor CHD4. EMBO J 29, 3130–3139. [PubMed: 20693977]

Price BD, and D'Andrea AD (2013). Chromatin remodeling at DNA double- strand breaks. Cell 152, 1344–1354. [PubMed: 23498941]

Pucella JN, Cols M, Yen WF, Xu S, and Chaudhuri J (2019). The B cell activation-induced miR-183 cluster plays a minimal role in canonical primary humoral responses. J. Immunol 202, 1383–1396. [PubMed: 30683701]

Qiao Q, Wang L, Meng FL, Hwang JK, Alt FW, and Wu H (2017). AID recognizes structured DNA for class switch recombination. Mol. Cell 67, 361–373.e4. [PubMed: 28757211]

Rada C, Di Noia JM, and Neuberger MS (2004). Mismatch recognition and uracil excision provide complementary paths to both Ig switching and the A/T-focused phase of somatic mutation. Mol. Cell 16, 163–171. [PubMed: 15494304]

Ramírez J, and Hagman J (2009). The Mi-2/NuRD complex: a critical epigenetic regulator of hematopoietic development, differentiation and cancer. Epi- genetics 4, 532–536.

Ramirez-Carrozzi VR, Nazarian AA, Li CC, Gore SL, Sridharan R, Im- balzano AN, and Smale ST (2006). Selective and antagonistic functions of SWI/SNF and Mi-2beta nucleosome remodeling complexes during an inflam- matory response. Genes Dev 20, 282–296. [PubMed: 16452502]

Rickert RC, Roes J, and Rajewsky K (1997). B lymphocyte-specific, Cre- mediated mutagenesis in mice. Nucleic Acids Res 25, 1317–1318. [PubMed: 9092650]

Robbiani DF, Bothmer A, Callen E, Reina-San-Martin B, Dorsett Y, Di- filippantonio S, Bolland DJ, Chen HT, Corcoran AE, Nussenzweig A, and Nussenzweig MC (2008). AID is required for the chromosomal breaks in c-myc that lead to c-myc/IgH translocations. Cell 135, 1028–1038. [PubMed: 19070574]

Robbiani DF, Bunting S, Feldhahn N, Bothmer A, Camps J, Deroubaix S, McBride KM, Klein IA, Stone G, Eisenreich TR, et al. (2009). AID pro- duces DNA double-strand breaks in non-Ig genes and mature B cell lym- phomas with reciprocal chromosome translocations. Mol. Cell 36, 631–641. [PubMed: 19941823]

Rouaud P, Saintamand A, Saad F, Carrion C, Lecardeur S, Cogné M, and Denizot Y (2014). Elucidation of the enigmatic IgD class-switch recombi- nation via germline deletion of the IgH 3′ regulatory region. J. Exp. Med 211, 975–985. [PubMed: 24752300]

Schrader CE, Bradley SP, Vardo J, Mochegova SN, Flanagan E, and Stavnezer J (2003). Mutations occur in the Ig Smu region but rarely in Sgamma regions prior to class switch recombination. EMBO J 22, 5893–5903. [PubMed: 14592986]

Sciammas R, Shaffer AL, Schatz JH, Zhao H, Staudt LM, and Singh H (2006). Graded expression of interferon regulatory factor-4 coordinates iso- type switching with plasma cell differentiation. Immunity 25, 225–236. [PubMed: 16919487]

Soneson C, Love MI, and Robinson MD (2015). Differential analyses for RNA-seq: transcript-level estimates improve gene-level inferences. F1000Res 4, 1521. [PubMed: 26925227]

Stanlie A, Aida M, Muramatsu M, Honjo T, and Begum NA (2010). His- tone3 lysine4 trimethylation regulated by the facilitates chromatin transcription complex is critical for DNA cleavage in class switch recombination. Proc. Natl. Acad. Sci. USA 107, 22190–22195. [PubMed: 21139053]

Teng G, and Schatz DG (2015). Regulation and evolution of the RAG recom- binase. Adv. Immunol 128, 1–39. [PubMed: 26477364]

Tessarz P, and Kouzarides T (2014). Histone core modifications regulating nucleosome structure and dynamics. Nat. Rev. Mol. Cell Biol 15, 703–708. [PubMed: 25315270]

Urquhart AJ, Gatei M, Richard DJ, and Khanna KK (2011). ATM medi- ated phosphorylation of CHD4 contributes to genome maintenance. Genome Integr 2, 1. [PubMed: 21219611]

Vakoc CR, Mandat SA, Olenchock BA, and Blobel GA (2005). Histone H3 lysine 9 methylation and HP1gamma are associated with transcription elongation through mammalian chromatin. Mol. Cell 19, 381–391. [PubMed: 16061184]

Vuong BQ, Herrick-Reynolds K, Vaidyanathan B, Pucella JN, Ucher AJ, Donghia NM, Gu X, Nicolas L, Nowak U, Rahman N, et al. (2013). A DNA break- and phosphorylation-dependent positive feedback loop promotes immunoglobulin class-switch recombination. Nat. Immunol 14, 1183–1189. [PubMed: 24097111]

Wang L, Wuerffel R, Feldman S, Khamlichi AA, and Kenter AL (2009). S region sequence, RNA polymerase II, and histone modifications create chro- matin accessibility during class switch recombination. J. Exp. Med 206, 1817–1830. [PubMed: 19596805]

Williams CJ, Naito T, Arco PG, Seavitt JR, Cashman SM, De Souza B, Qi X, Keables P, Von Andrian UH, and Georgopoulos K (2004). The chromatin remodeler Mi-2beta is required for CD4 expression and T cell devel- opment. Immunity 20, 719–733. [PubMed: 15189737]

Xu Z, Fulop Z, Wu G, Pone EJ, Zhang J, Mai T, Thomas LM, Al-Qah- tani A, White CA, Park SR, et al. (2010). 14-3-3 adaptor proteins recruit AID to 5'-AGCT-3'-rich switch regions for class switch recombination. Nat.Struct. Mol. Biol 17, 1124–1135. [PubMed: 20729863]

Xu Z, Zan H, Pone EJ, Mai T, and Casali P (2012). Immunoglobulin class-switch DNA recombination: induction, targeting and beyond. Nat. Rev. Immunol 12, 517–531. [PubMed: 22728528]

Yewdell WT, and Chaudhuri J (2017). A transcriptional serenAID: the role of noncoding RNAs in class switch recombination. Int. Immunol 29, 183–196. [PubMed: 28535205]

Yoshida T, Hazan I, Zhang J, Ng SY, Naito T, Snippert HJ, Heller EJ, Qi X, Lawton LN, Williams CJ, and Georgopoulos K (2008). The role of the chromatin remodeler Mi-2beta in hematopoietic stem cell self-renewal and multilineage differentiation. Genes Dev 22, 1174–1189. [PubMed: 18451107]

Young MD, Wakefield MJ, Smyth GK, and Oshlack A (2010). Gene Ontology analysis for RNA-seq: accounting for selection bias. Genome Biol 11, R14. [PubMed: 20132535]

Yu K, and Lieber MR (2003). Nucleic acid structures and enzymes in the immunoglobulin class switch recombination mechanism. DNA Repair (Amst.) 2, 1163–1174. [PubMed: 14599739]

Zan H, and Casali P (2015). Epigenetics of peripheral B-cell differentiation and the antibody response. Front. Immunol 6, 631. [PubMed: 26697022]

Zheng S, Vuong BQ, Vaidyanathan B, Lin JY, Huang FT, and Chaud- huri J (2015). Non-coding RNA generated following lariat debranching mediates targeting of AID to DNA. Cell 161, 762–773. [PubMed: 25957684]

Zilfou JT, and Lowe SW (2009). Tumor suppressive functions of p53. Cold Spring Harb. Perspect. Biol 1, a001883. [PubMed: 20066118]

Ziv Y, Bielopolski D, Galanty Y, Lukas C, Taya Y, Schultz DC, Lukas J, Bekker-Jensen S, Bartek J, and Shiloh Y (2006). Chromatin relaxation in response to DNA double-strand breaks is modulated by a novel ATM- and KAP-1 dependent pathway. Nat. Cell Biol 8, 870–876. [PubMed: 16862143]

Highlights

- CHD4 is essential for early B cell development
- Naive, mature B cells can sustain loss of CHD4
- CHD4 represses p53 expression and promotes B cell proliferation
- Loss of CHD4 influences recruitment of AID to the Igh locus and impairs CSR

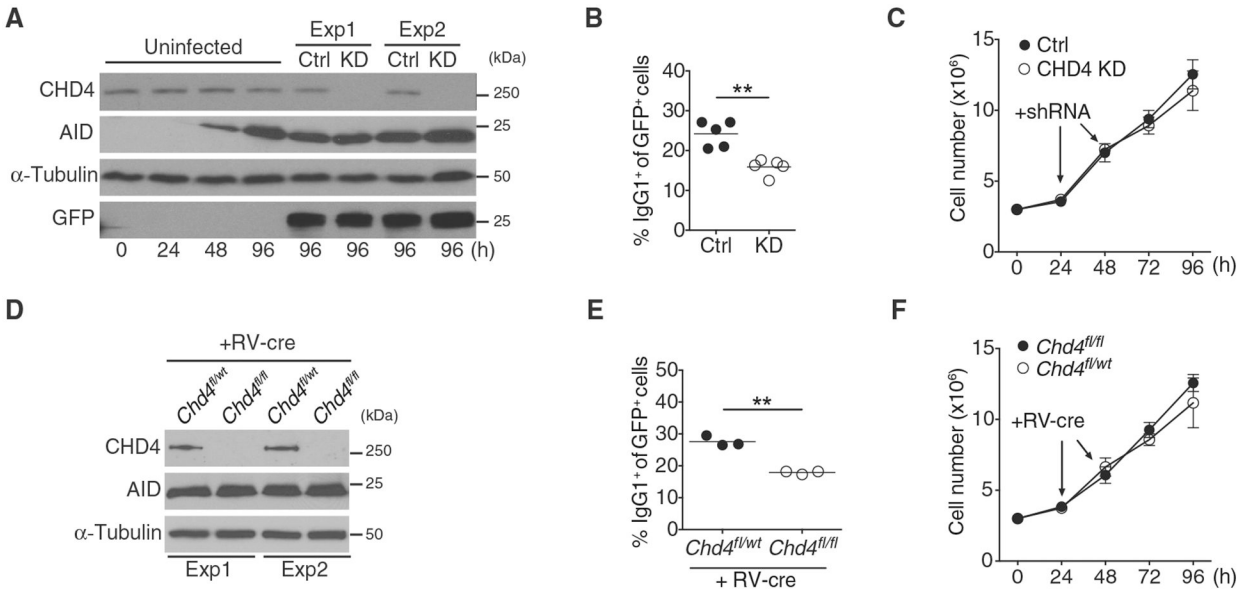

Figure 1. CHD4 Depletion Impairs CSR

(A) CHD4 expression in B cells. Splenic B cells stimulated with LPS plus IL-4 were either uninfected or retrovirally infected with vector expressing shRNA directed toward CHD4 (KD) or non-specific, scrambled control (Ctrl). The retroviral vector also expresses GFP to allow detection of transduced cells. Cells were harvested at indicated time points, whole-cell protein extracts were prepared and analyzed on immunoblots using indicated antibodies. a-Tubulin was used as a loading control, while GFP served as a control for retroviral transduction. Immunoblot is representative of two independent experiments.

(B) shRNA-mediated depletion of CHD4 impairs CSR. Frequency of CSR to IgG1 was determined using flow cytometry. Frequency of $IgG1^+$ cells within the GFP^+ gate at 96 h post-stimulation from five independent experiments is shown (**$p < 0.005$).

(C) Growth of control and CHD4-depleted cells. Splenic B cells (3×10^6 per well) transduced with Ctrl or CHD4 shRNA were counted at different time points. Each point in the growth curve represents the average (mean ± SD) of five independent experiments.

(D) Cre-mediated deletion of CHD4. *Chd4*$^{fl/fl}$ and control (*Chd4*$^{fl/wt}$) splenic B cells stimulated with LPS plus IL-4 were transduced with retroviral vector (RV-cre) expressing cre recombinase and GFP. Whole-cell extracts were prepared at 96 h and analyzed on immunoblots using antibodies against CHD4, AID, or α-tubulin (loading control). Immunoblot is representative of two independent experiments.

(E) CSR is impaired in CHD4 deleted B cells. *Chd4*$^{fl/fl}$ and control (*Chd4*$^{fl/wt}$) splenic B cells transduced with cre-recombinase was determined by flow cytometry. CSR to $IgG1^+$ cells within the GFP^+ gate from three independent experiments are shown (**$p < 0.005$) (right).

(F) Growth of CHD4-deleted B cells. Cells were counted as described in (C). Each point on the growth curve represents the average (mean ± SD) of three in- dependent experiments.

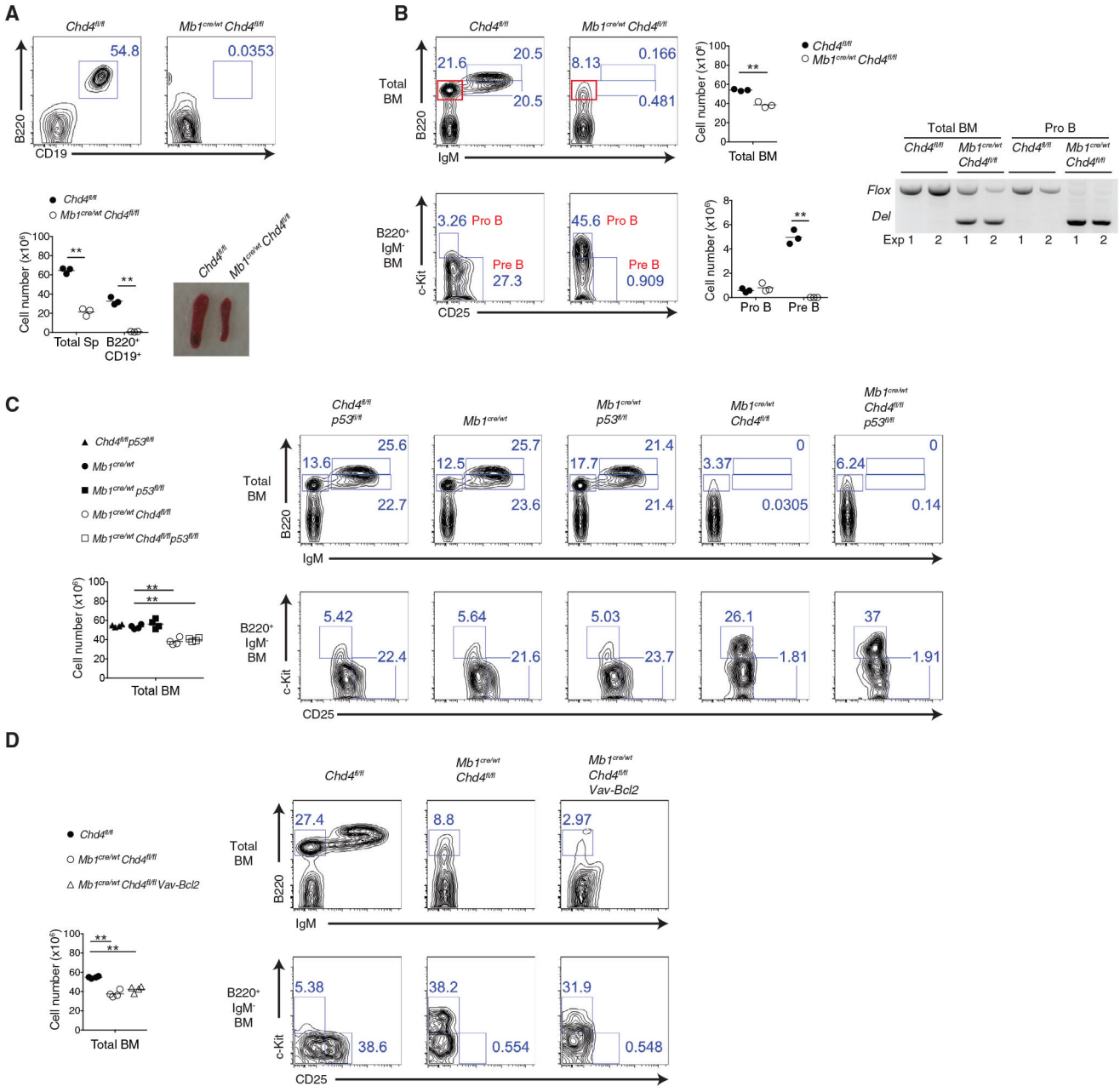

Figure 2. CHD4 Is Essential for Early B Cell Development

(A) Mature B cells are absent in spleens of *Mb1*$^{cre/wt}$*Chd4*$^{fl/fl}$ mice. Splenocytes were stained with B220 and CD19 and analyzed using flow cytometry (top panel). Absolute numbers of total splenocytes and CD19^{+} B220^{+} B cells from each mouse strain are shown (n = 3; **p < 0.005) (bottom left). The spleen from a representative 10-week-old *Mb1*$^{cre/wt}$*Chd4*$^{fl/fl}$ mouse was compared with littermate control (*Chd4*$^{fl/fl}$) (bottom right). (B) CHD4 deletion impairs early B cell development in the bone marrow. Flow cytometric analysis shows expression of IgM and B220 in the bone marrow. Cellularity of bone marrow is shown on the right side of representative flow plots. BM cells were stained with c-Kit and CD25 and analyzed for pre-B (IgM^{-} B220^{+} CD25^{+} c-Kit^{-}) and pro-B (IgM^{-} B220^{+} CD25^{-}

c-Kit^{+}) cells. The red box represents the parent gate for analysis of pre-B and pro-B cells. n = 5; **p < 0.005. Furthermost right panel shows PCR-based genotyping and loss of the fl cel *Chd4* allele in total bone marrow cells and sorted pro-B cells. Genotyping PCR from two independent experiments is shown.

(C) Loss of p53 does not restore B cell developmental defects in *Mb1*$^{cre/wt}$*Chd4*$^{fl/fl}$ mice. Absolute numbers of bone marrow from each mouse strain are shown (n = 4; **p < 0.005) (left). Flow cytometric analysis shows expression of IgM and B220 expression or CD25 and c-Kit in bone marrow (BM) (right).

(D) Transgenic expression of Bcl2 does not rescue B cell developmental defects in *Mb1*$^{cre/wt}$*Chd4*$^{fl/fl}$ mice. Absolute numbers of total bone marrow from each mouse strain are shown (left) (n = 4; **p < 0.005). Flow cytometric analysis shows IgM and B220 expression or CD25 and c-Kit expression in total bone marrow (BM) (right).

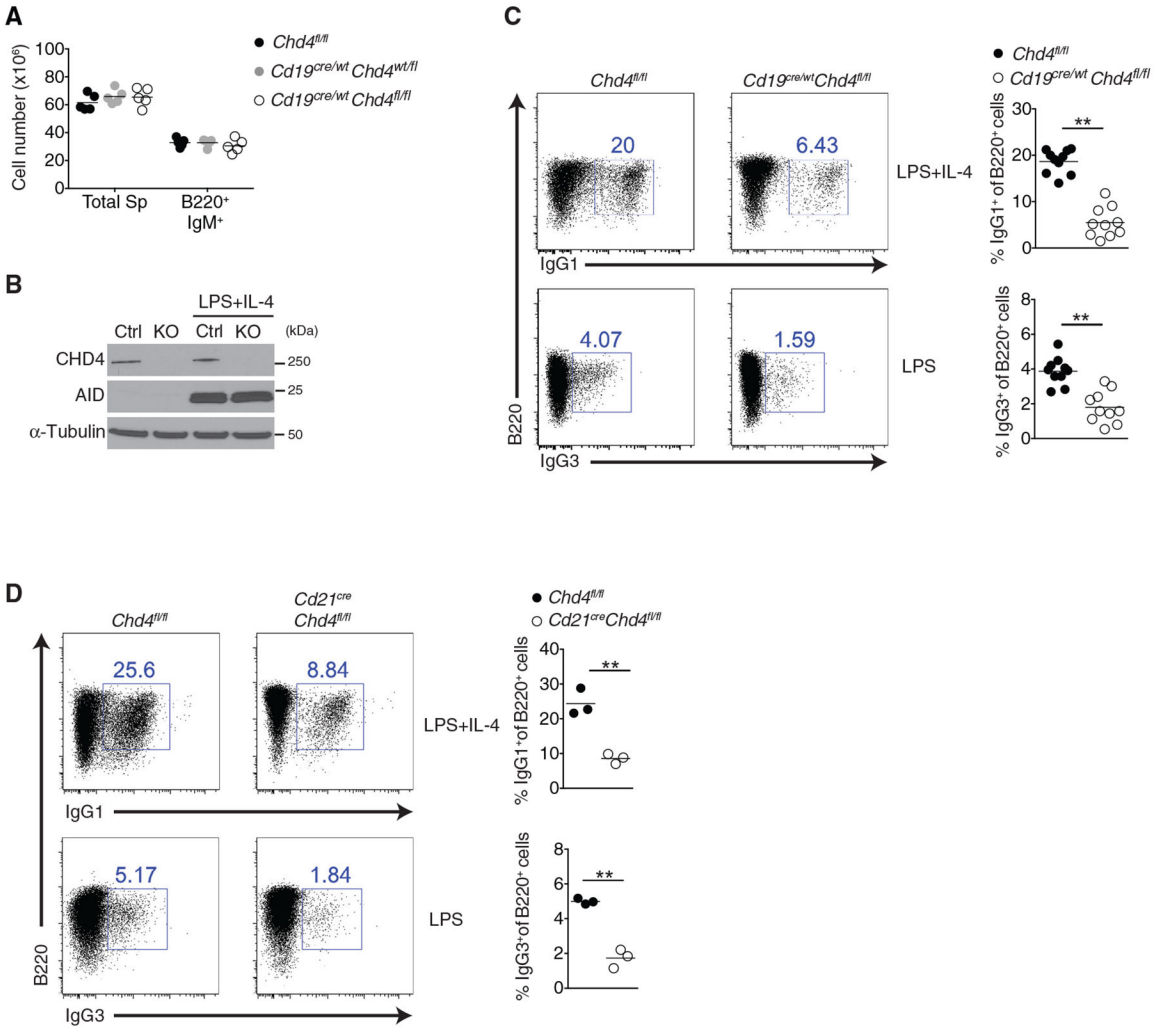

Figure 3. CHD4 Is Required for Efficient CSR *Ex Vivo*

(A) CD19-cre-mediated deletion of CHD4 does not affect splenic B cell numbers. Absolute numbers of total splenocytes and IgM^+ $B220^+$ B cells from indicated littermates are shown (n = 5).

(B) Loss of CHD4 protein in CHD4 KO mice. Whole-cell extracts derived from stimulated CHD4 KO (*Cd19*$^{cre/wt}$*Chd4*$^{fl/fl}$) and control (*Chd4*$^{fl/fl}$) B cells were analyzed on immunoblots. Immunoblot is representative of two independent experiments.

(C) CHD4 loss impairs CSR. B cells were stimulated for 96 h with LPS plus IL-4 for IgG1 switching or with LPS alone for IgG3 switching. Representative flow cytometric plots are shown (left). Frequency of class-switched cells is indicated (n = 10; **p < 0.005) (right).

(D) CHD4 deletion using CD21-cre also impairs CSR. Splenic B cells from *Chd4*$^{fl/fl}$ and *Cd21*^{cre}*Chd4*$^{fl/fl}$ mice were stimulated with LPS plus IL-4 or LPS alone and CSR to IgG1 or IgG3 was analyzed using flow cytometry. A representative plot is shown (left), and the frequency of CSR is quantified (n = 3; **p < 0.005) (right).

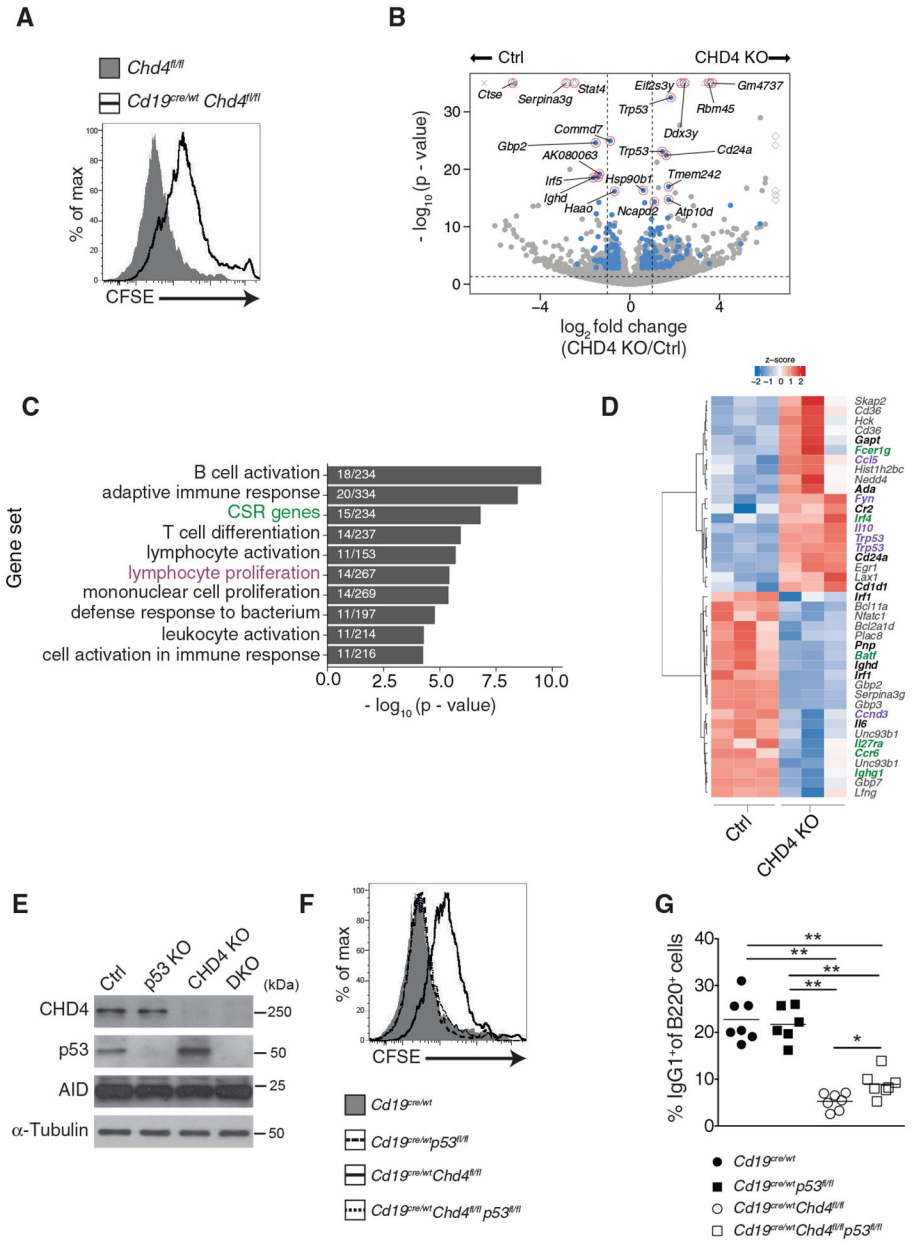

Figure 4. CHD4 Promotes B Cell Proliferation

(A) Analysis of cell proliferation using CFSE stain- ing. CFSE-labeled CDH4 KO (*Cd19*$^{cre/wt}$*Chd4*$^{fl/fl}$) and control (*Chd4*$^{fl/fl}$) splenic B cells were cultured for 96 h after LPS plus IL-4 stimulation. Dilution of CFSE was examined using flow cytometry.

(B) Volcano plot of RNA sequencing (RNA-seq) data showing $\log_2$ fold change on x axis and $-\log_{10}$ (p value) on y axis of splenic B cells after LPS plus IL-4 stimulation for 48 h. Blue dots indicate differentially expressed (DE) transcripts (false discovery rate [FDR] < 0.05, $|\log_2$ fold change$| > 0.5$, transcripts per million [TPM] > 10). Diamonds, triangles, and crosses depict values that extend beyond the fold change, p value, or both axes, respectively. Top 20 significant DE transcripts are highlighted. Dotted lines mark p value = 0.05 and $\log_2$ fold change = ±1.

(C) Bar plots display $-\log_{10}$(p value) of gene set enrichment tests calculated from highly expressed DE genes. Fraction of DE genes out of total number of gene set genes are displayed within each bar.

(D) Heatmap of DE transcripts of genes found within gene sets displayed in (C). Genes high- lighted in green indicate CSR genes, purple indicates lymphocyte proliferation genes, and black indicates those genes shared between both gene sets.

(E) Whole-cell extracts derived from splenic B cells from control (*Cd19*$^{cre/wt}$), p53KO(*Cd19*$^{cre/wt}$*p53*$^{fl/fl}$), CHD4 KO (*Cd19*$^{cre/wt}$*Chd4*$^{fl/fl}$),and DKO (*Cd19*$^{cre/wt}$*Chd4*$^{fl/fl}$*p53*$^{fl/fl}$) mice stimulated in culture with LPS plus IL-4 for 96 h were analyzed on immunoblots. Immunoblot is representative of two independent experiments.

(F) Analysis of cell proliferation by CFSE staining. Splenic B cells derived from mice of the indicated genotypes were stained with CFSE and cultured for 96 h with LPS plus IL-4.

(G) IgG1 surface expression by flow cytometry in B cells derived from mice of the indicated genotypes. B cells were stimulated with LPS plus IL-4 for 96 h and examined for CSR to IgG1. Quantification of frequency of switched cells is indicated in each plot (n = 6; *p < 0.05 and **p < 0.005).

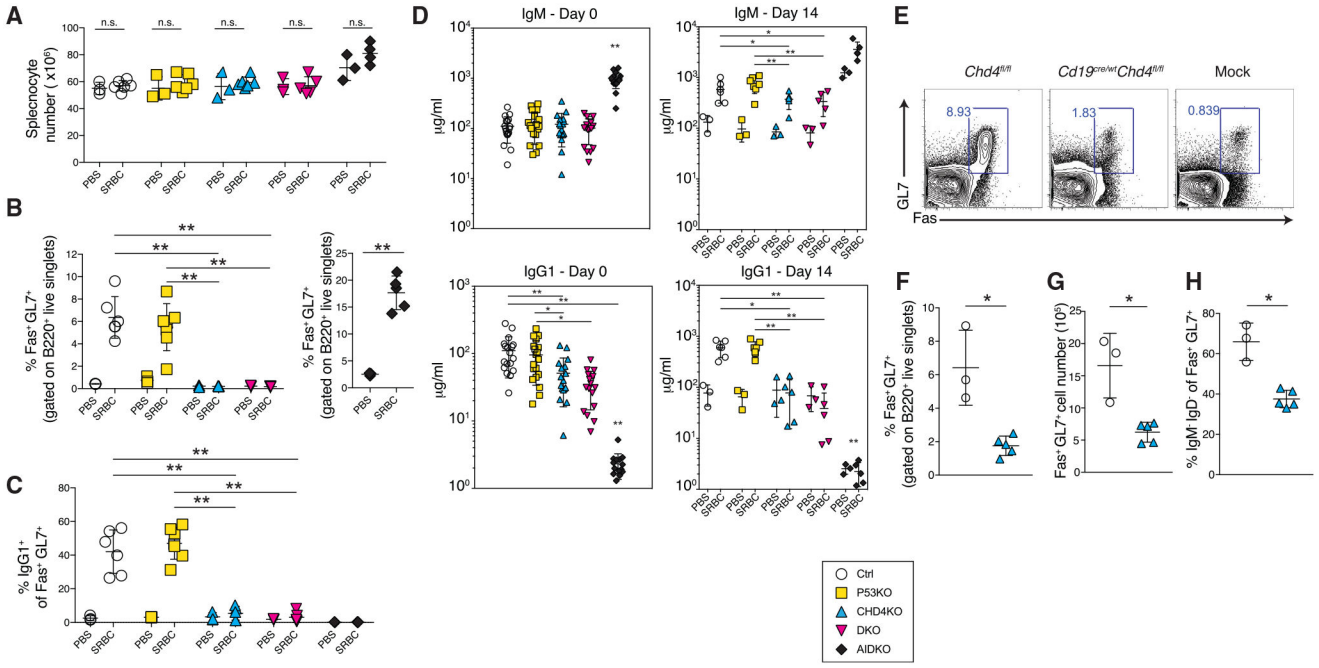

Figure 5. CHD4 Influences Germinal Center Formation and IgG1 CSR *In Vivo*

(A–D) Mice were immunized with 1×10^8 packed sheep red blood cells (SRBCs) or PBS (mock), boosted at d10, and analyzed at d14.

((A) Splenocyte number at d14 after SRBC or mock immunization.

(B) Frequency of germinal center (GC) B cells (Fas^+ $GL7^+$ of $B220^+$ splenocytes) in the spleen at d14 post-immunization. The right panel shows frequency of GC B cells in *Aicda*$^{-/-}$ mice.

(C) Frequency of $IgG1^+$ among GC B cells ($IgG1^+$ of Fas^+ $GL7^+$ $B220^+$) in the spleen at d14.

(D) IgM and IgG1 levels in the serum at d0 or d14 after SRBC immunization were analyzed using ELISA. Mice used in the analysis: control (*Cd19*$^{cre/wt}$), p53KO (*Cd19*$^{cre/wt}$*p53*$^{fl/fl}$), CHD4 KO (*Cd19*$^{cre/wt}$*Chd4*$^{fl/fl}$), DKO (*Cd19*$^{cre/wt}$*Chd4*$^{fl/fl}$*p53*$^{fl/fl}$), and AID KO (*Aicda*$^{-/-}$). For (A)–(D), n = 3 for PBS, n = 6 for SRBC immunization; *p < 0.05 and **p < 0.005.

(E–H) Mice were immunized with 50 mg NP-CGG in alum or with PBS (mock), boosted at d10 post-immunization with 50 mg of NP-CGG in alum, and B cells in the spleen were analyzed at d14 post-immunization.

(E) Representative flow cytometry plot of GC B cells (Fas^+ $GL7^+$ of $B220^+$ splenocytes) in spleens of NP-CGG or mock immunized mice.

(F) Frequency of GC B cells at d14 post-immunization ($GL7^+$ Fas^+ of $B220^+$ cells).

(G) Absolute number of GC B cells at d14 post-immunization ($B220^+$ Fas^+ $GL7^+$).

(H) Frequency of class-switched GC B cells (IgM^- IgD^- of Fas^+ $GL7^+$ of $B220^+$) at d14 post-immunization.

Mice used for (E)–(H), control, *Chd4*$^{fl/fl}$, n = 3; CHD4 KO (*Cd19*$^{cre/wt}$*Chd4*$^{fl/fl}$), n = 5; *p < 0.05.

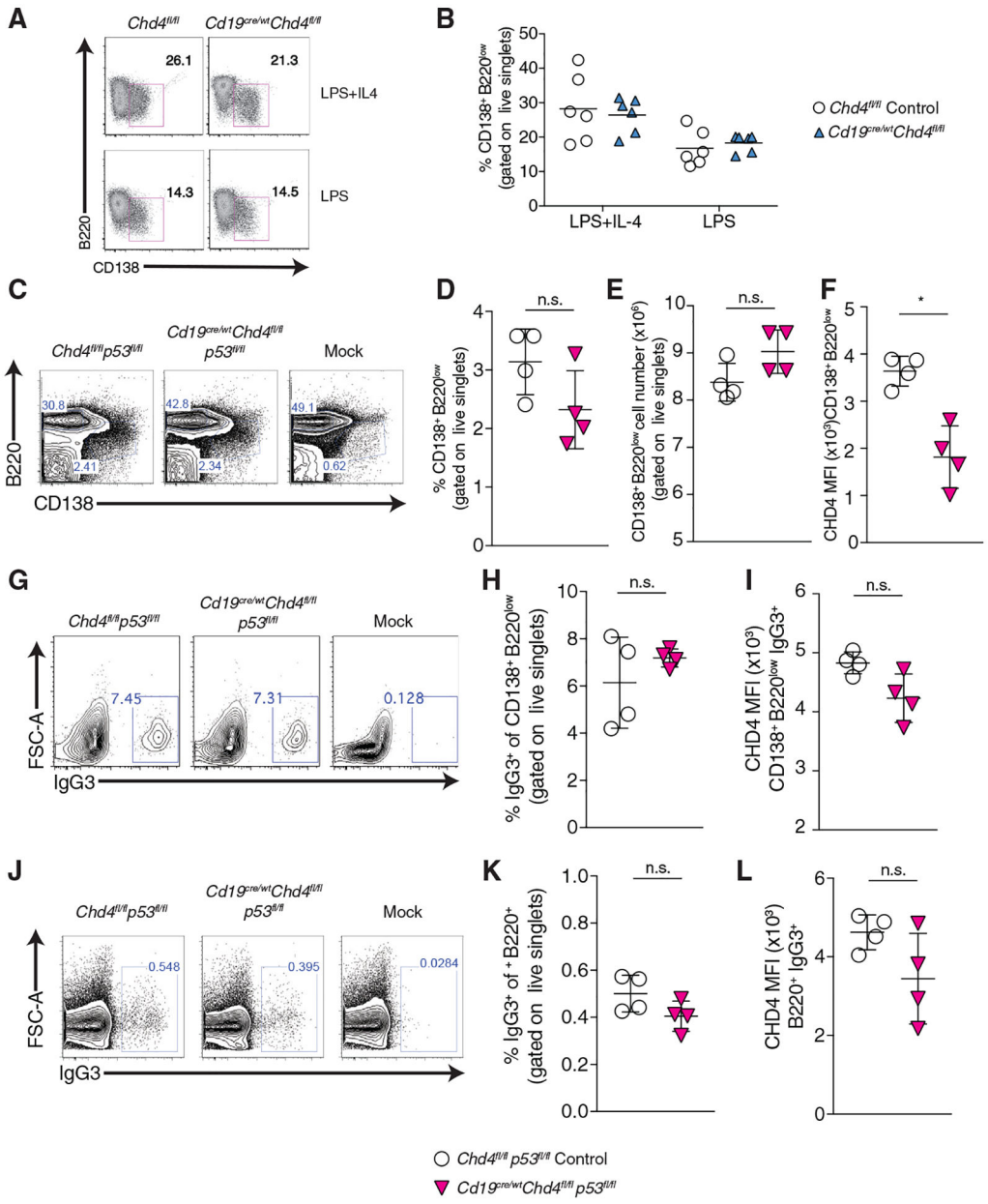

Figure 6. CHD4 Is Dispensable for Plasma-blast Differentiation

(A and B) Naive splenic B cells from control (*CHD4*$^{fl/fl}$) or CHD4 KO (*Cd19*$^{cre/wt}$*Chd4*$^{fl/fl}$) mice were stimulated *in vitro* with LPS alone or LPS plus IL-4 for 96 h, and formation of B220^{lo} CD138^{+} plasmablasts was examined.

(A) Representative flow cytometry data.

(B) Frequency of B220^{lo} CD138^{+} plasmablast for- mation *in vitro* (n = 5).

(C–L) Mice were intravenously injected with 50 mg LPS or PBS (mock) and analyzed at day 5.

(C) Representative flow cytometry plot for B220^{lo} CD138^{+} plasmablasts. Mock represents *Chd4*$^{fl/fl}$*p53*$^{fl/fl}$ animals injected with PBS.

(D) Frequency of plasmablasts (B220^{lo} CD138^{+} of live cells).

(E) Absolute number of plasmablasts ($B220^{lo}$ $CD138^{+}$ live cells).
(F) Intracellular staining of CHD4 within plasma- blast population ($B220^{lo}$ $CD138^{+}$ of live cells).
(G) Representative flow cytometry plot of IgG3 intracellular staining of $B220^{lo}$ $CD138^{+}$ live cell population. Mock represents $Chd4^{fl/fl}p53^{fl/fl}$ animals injected with PBS.
(H) Frequency of $IgG3^{+}$ plasmablasts (amongst $B220^{lo}$ $CD138^{+}$ live cells).
(I) MFI of CHD4 expression in IgG3 positive plasmablasts. (J) Representative flow cytometry plot for IgG3 cells within the $B220^{+}$ live cell population. Mock represents $Chd4^{fl/fl}p53^{fl/fl}$ animals injected with PBS.
(K) Frequency of IgG3 CSR upon LPS administration among total $B220^{+}$ cells.
(L) Intracellular staining of CHD4 in IgG3-positive B cells.
Mice used in (C–L): n = 3 control ($Chd4^{fl/fl}$),n = 5 CHD4 KO ($Cd19^{cre/wt}Chd4^{fl/fl}$); n = 4 control ($Chd4^{fl/lf}p53^{fl/fl}$), n = 4 DKO ($Cd19^{cre/wt}Chd4^{fl/fl}p53^{fl/fl/}$). *$p < 0.005$.

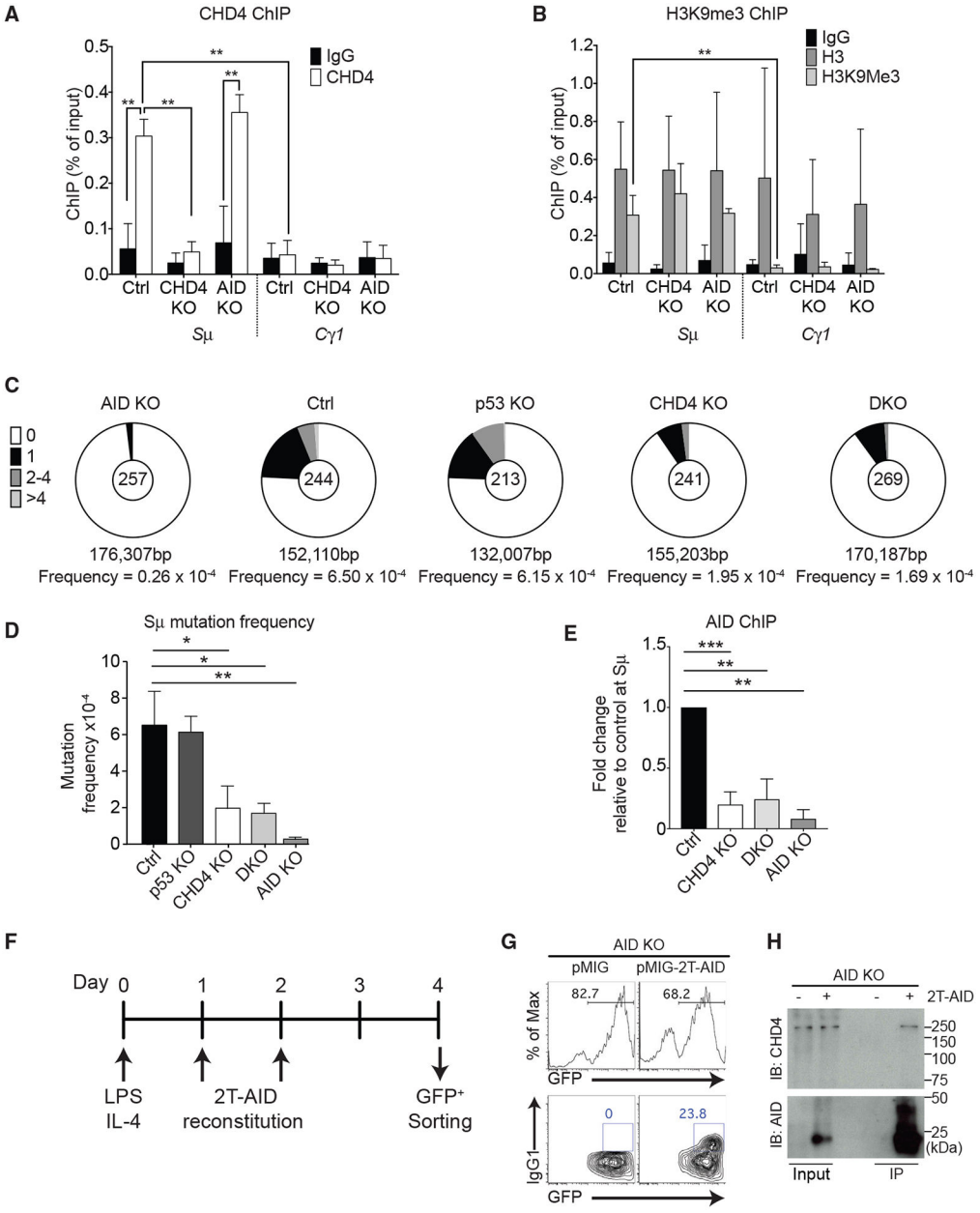

Figure 7. CHD4 Mediates Localization of AID to Switch Region DNA

(A) CHD4 binds to Sm. ChIP analysis was performed on chromatin prepared from LPS plus IL-4-stimulated (48 h) splenic B cells harvested from control (*Cd19*$^{cre/wt}$), CHD4 KO (*Cd19*$^{cre/wt}$*Chd4*$^{fl/fl}$), or *Aicda*$^{-/-}$ mice. Quantification of ChIP signals at Sμ and Cγ (negative control) is indicated in each plot as percentage of input (mean ± SD) (n = 6; **p < 0.005).

(B) H3K9me3 epigenetic mark is present at Sm. Splenic B cells harvested from mice of the indicated genotypes were stimulated with LPS plus IL-4 for 48 h, and ChIP analysis was performed using antibodies specific for H3K9me3. ChIP using histone H3 antibodies and non-specific IgG served as positive and negative controls, respectively. Quantification of ChIP signal is indicated as percent of input (mean ± SD) (n = 6; **p < 0.005).

(C) Loss of CHD4 reduces frequency of 5'-Sμ mutations. Splenic B cells from control (*Cd19*$^{cre/wt}$), p53 KO (*Cd19*$^{cre/wt}$*p53*$^{fl/fl}$), CHD4 KO (*Cd19*$^{cre/wt}$*Chd4*$^{fl/fl}$), DKO (*Cd19*$^{cre/wt}$*Chd4*$^{fl/fl}$*p53*$^{fl/fl}$), and AID KO (*Aicda*$^{-/-}$) were activated *ex vivo* for 96 h with LPS plus IL-4, and the 5'-Sμ region was PCR amplified and sequenced.B cells from AID KO mice served as control to estimate the frequency of PCR error. Pie charts illustrate the fraction of sequences with the indicated number of mutations; total number of sequences analyzed is shown at the center of each chart; total number of base pairs (bp) sequenced and average mutation rate is shown beneath each chart.

(D) Quantification of mutation frequency per bp at 5'-Sμ. Data are from three independent experiments (mean ± SD) (n = 3; *$p < 0.05$ and **$p < 0.005$).

(E) ChIP analysis for AID occupancy at the Sm in control (*Cd19*$^{cre/wt}$), CHD4 KO (*Cd19*$^{cre/wt}$*Chd4*$^{fl/fl}$), DKO (*Cd19*$^{cre/wt}$*Chd4*$^{fl/fl}$*p53*$^{fl/fl}$), and *Aicda*$^{-/-}$ activated B cells at 72 h after LPS plus IL-4 stimulation. ChIP values for AID were normalized to control (*Cd19*$^{cre/wt}$) and plotted (mean ± SD) (n = 3; *$p < 0.05$ and **$p < 0.005$).

(F) Scheme to assess interaction between AID and CHD4. AID KO splenic B cells were retrovirally transduced with HA-FLAG-AID (2T-AID) via a vector expressing GFP. Cells expressing GFP were sorted at 96 h post-LPS plus IL-4 stimulation.

(G) 2T-AID restores CSR in AID KO B cells. Frequency of CSR to IgG1 was assessed 96 h after B cell harvest.

(H) AID forms a complex with CHD4. Whole-cell extracts expressing pMIG-2T-AID or control (pMIG) B cells were immunoprecipitated with HA antibodies and analyzed on immunoblots using CHD4 or AID antibodies. Immunoblot is representative of two independent experiments.

KEY RESOURCES TABLE

REAGENT or RESOURCE	SOURCE	IDENTIFIER
Antibodies		
Mouse monoclonal anti α-tubulin	Sigma	Cat# T19026; RRID: AB_477593
Rabbit monoclonal anti-CHD4	Cell Signaling Technology	Cat#11912; RRID: AB_2751014
Mouse monoclonal anti-CHD4	Abcam	Cat# ab70469; RRID: AB_2229454
Rabbit polyclonal anti-H3	Abcam	Cat# ab1791; RRID: AB_302613
Rabbit polyclonal anti-H3K9me3	Abcam	Cat# ab8898; RRID: AB_306848
Goat polyclonal anti-p53	Santa Cruz Biotechnology	Cat# sc-6243-G; RRID: AB_653754
Rat monoclonal anti-B220 BV510	BioLegend	Cat# 103247; RRID:AB_2561394
Rat monoclonal anti-B220 FITC	BD Biosciences	Cat# 553088; RRID: AB_394618
Rat monoclonal anti-B220 PerCP Cyanine 5.5	Thermo Fisher Scientific	Cat# 45-0452-82; RRID: AB_1107006
Rat monoclonal anti-B220 PE-Cy7	BD Biosciences	Cat# 552772; RRID: AB_394458
Rat monoclonal anti-B220 AF700	Thermo Fisher Scientific	Cat# 56-0452-82; RRID: AB_891458
Rat monoclonal anti-B220 APC/eF780	Thermo Fisher Scientific	Cat# 47-0452-80; RRID: AB_1518811
Rat monoclonal anti-CD3 BUV737	BD Biosciences	Cat# 564380; RRID: AB_2738781
Rat monoclonal anti-CD19 PerCP-Cyanine 5.5	Thermo Fisher Scientific	Cat# 45-0193-82; RRID: AB_I106999
Rat monoclonal anti-CD19 PE	BD Biosciences	Cat# 557399; RRID: AB_396682
Rat monoclonal anti-CD19 PE-Cyanine7	Thermo Fisher Scientific	Cat# 25-0193-81; RRID: AB_65766
Rat monoclonal anti-CD25 PE-Cyanine7	BD Biosciences	Cat# 552880; RRID: AB_394509
Rat monoclonal anti-CD25 APC-eF780	Thermo Fisher Scientific	Cat# 47-0251-82; RRID: AB_I272179
Armenian hamster monoclonal anti-CD95 BV510	BD Biosciences	Cat# 563646; RRID: AB_2738345
Mouse monoclonal anti-CHD4 PE	Novus	Cat# NBP2-50163PE; N/A
Rat monoclonal Anti-Mouse CD117 (c-Kit) APC	Thermo Fisher Scientific	Cat# 17-1171-82; RRID: AB_469430
Rat monoclonal Anti-Mouse CD117 (c-Kit) PE	Thermo Fisher Scientific	Cat# 12-1171-82; RRID:AB_465813
DAPI	Invitrogen	Cat#D1306; RRID: AB_2307445
Rat monoclonal Anti-GL7 FITC	BD Biosciences	Cat# 553666; RRID: AB_394981
Rat monoclonal Anti-GL7 eFluor450	Thermo Fisher Scientific	Cat# 48-5902-82; RRID: AB_10870775
Rat monoclonal Anti-IgA PE	Thermo Fisher Scientific	Cat# 12-4204-83; RRID: AB_465918
IgA antibody	SouthernBiotech	Cat# 1040-01; RRID: AB_2314669
Mouse monoclonal IgA antibody	BD Biosciences	Cat# 553476; RRID:AB_479590
Goat Anti-Mouse IgA-HRP antibody	SouthernBiotech	Cat# 1040-05; RRID:AB_2714213
Rat monoclonal Anti-IgD AF700	BioLegend	Cat# 405729; RRID:AB_2563340
Rat monoclonal Anti-IgGI APC	BD Biosciences	Cat# 550874; RRID:AB_398470
Goat polyclonal Anti-Mouse IgG1	SouthernBiotech	Cat# 1070-01; RRID: AB_2794408
Mouse monoclonal IgG1	SouthernBiotech	Cat# 0102-01; RRID: AB_2793845
Goat polyclonal Anti-mouse IgG1	SouthernBiotech	Cat# 1070-05; RRID: AB_2650509
Rat monoclonal Anti-IgG3 FITC	BD Biosciences	Cat# 553403; RRID: AB_394840
Rat monoclonal Anti-IgM FITC	BD Biosciences	Cat# 553408; RRID: AB_394844
Rat monoclonal Anti-IgM eF450	Thermo Fisher Scientific	Cat# 48-5790-82; RRID: AB_2574073
Rat monoclonal Anti-IgM PE	Thermo Fisher Scientific	Cat# 12-5790-81; RRID: AB_465939
Rat monoclonal mouse IgM APC-eF780	Thermo Fisher Scientific	Cat# 47-5790-82; RRID: AB_2573984

REAGENT or RESOURCE	SOURCE	IDENTIFIER
Rat monoclonal Anti-IgM BUV395	BD Biosciences	Cat# 743329; RRID: AB_2741430
Goat polyclonal Anti-Mouse IgG1	SouthernBiotech	Cat# 1070-01; RRID: AB_2794408
Mouse IgM isotype control	Thermo Fisher Scientific	Cat# 14-4752-81; RRID: AB_470122
Goat polyclonal Anti-IgM	SouthernBiotech	Cat# 1020-05; RRID:AB_2794201
Hamster monoclonal Anti-CD40	Thermo Fisher Scientific	Cat# 16-0402-82; RRID: AB_468945
Rabbit polyclonal Anti-AID	Chaudhuri et al., 2003	N/A
Bacterial and Virus Strains		
MSCV-Cre	Addgene	Plasmid# 24064
Biological Samples		
Sheep Red Blood cells	Innovative Research	Cat# IC100-0210
Chemicals, Peptides, and Recombinant Proteins		
NP-PE	Biosearch Technologies	Cat# N-5070-1
NP-CGG	Biosearch Technologies	Cat# N-5055D-5
Zombie Red viability dye	BioLegend	Cat# 423109
Trizol	Invitrogen	Cat# 15596026
LPS	Sigma-Aldrich	Cat#L4130
IL-4	R&D Systems	Cat#404-ML-100
IL-5	Peprotech	Cat#215-15
TGF-β	Fischer Scientific	Cat#240-B-010
Retinoic acid	Sigma-Aldrich	Cat#R2625-50-MG
BAFF	AdipoGen Life Sciences	Cat#AG-40B-0022-3010
IFN-γ	Gemini Bio-Products	Cat#300-311P
IL-21	R&D Systems	Cat#594-ML-010
Cell Trace CFSE	Thermo Fisher Scientific	*Cat# C34554*
LPS from *Salmonella minnesota* R595	Enzo LifeSciences	Cat# ALX-581–008-L002
SYBR Green master mix	Applied Biosystems	Cat#A25741
Critical Commercial Assays		
ChIP assay kit	Millipore Sigma	Cat#17-295
RNeasy mini kit	QIAGEN	Cat#74104
SMART-Seq v4 Ultra Low Input RNA Kit	Clontech	Cat#63488
KAPA Hyper Prep Kit	Kapa Biosystems	Cat#KK8504
Deposited Data		
RNA-seq	This paper	https://www.ncbi.nlm.nih.gov/geo/query/acc.cgi?acc=GSE128321
Experimental Models: Cell Lines		
HEK293T	ATCC	Cat#ATCC® CRL-3216
Experimental Models: Organisms/Strains		
C57BL/6 mice	Jackson labs	Cat# JAX: 000664
CHD4 fl/fl	Williams et al., 2004	N/A
$Aicda^{-/-}$	Muramatsu et al., 2000	N/A
$Mb1^{cre/cre}$	Hobeika et al., 2006	N/A
$Aicda^{cre/cre}$	Robbiani et al., 2008	N/A
CD19-Cre	Jackson labs	Cat# JAX: 006785

REAGENT or RESOURCE	SOURCE	IDENTIFIER
CD21-Cre	Jackson labs	Cat# JAX: 006368
Vav-Bcl2	Egle et al., 2004	N/A
p53 fl/fl	Jackson labs	Cat# JAX: 008462
Oligonucleotides		
S 5′-TGCGTGACATCAAAGAGAAG-3′ Actb	This paper	N/A
AS 5′-CGGATGTCAACGTCACACTT-3′ Actb	This paper	N/A
S 5′-TAGTAAGCGAGGCTCTAAAAAGCAT-3′ μ-GLT	This paper	N/A
AS 5′-AGAACAGTCCAGTGTAGGCAGTAGA-3′ μ-GLT	This paper	N/A
S 5′-GGCCCTTCCAGATCTTTGAG-3′ γ1-GLT	This paper	N/A
AS 5′-GGATCCAGAGTTCCAGGTCACT-3′ γI-GLT	This paper	N/A
S 5′-TAAAATGCGCTAAACTGAGGTGATTACT-3′ Sm	This paper	N/A
AS 5′-CATCTCAGCTCAGAACAGTCCAGTG-3′ Sm	This paper	N/A
S 5′-GCACACAGCTCAGACGCAACC-3′ CCA	This paper	N/A
AS 5′ -TGGTCAGCACAGAGGTCACGGA-3′ CTG	This paper	N/A
Software and Algorithms		
R (v.3.3.3)	https://cran.r-project.org/	https://cran.r-project.org/
Trimmomatic (v.0.36)	Bolger et al., 2014	http://www.usadellab.org/cms/?page=trimmomatic
Salmon (v0.8.2)	Patro et al., 2017	https://salmon.readthedocs.io/en/latest/index.html
tximport (v.1.8.0)	Soneson et al., 2015	https://bioconductor.org/packages/release/bioc/html/tximport.html
DESeq2 (v.1.14.1)	Love et al., 2014	http://bioconductor.org/packages/release/bioc/html/DESeq2.html
GOseq (v.1.26.0)	Young et al., 2010	https://bioconductor.org/packages/release/bioc/html/goseq.html
Prism 7	GraphPad software Inc.	N/A
FlowJo 9.9	FloJo LLC	N/A
Other		
CD43 (Ly-48) MicroBeads	Miltenyi Biotec	Cat# 130-049-801